Cyclophane-Type Fullerene-dibenzo[18]crown-6 Conjugates with *trans-1*, *trans-2*, and *trans-3* Addition Patterns: Regioselective Templated Synthesis, X-Ray Crystal Structure, Ionophoric Properties, and Cation-Complexation-Dependent Redox Behavior

by **Jean-Pascal Bourgeois**, **Paul Seiler**, **Monia Fibbioli**, **Ernö Pretsch***, **François Diederich**[1])*

Laboratorium für Organische Chemie, ETH-Zentrum, Universitätstrasse 16, CH-8092 Zürich

and **Luis Echegoyen***

Department of Chemistry, University of Miami, Coral Gables, FL 33124, USA

The fullerene-crown ether conjugates (±)-**1** to (±)-**3** with *trans-1* ((±)-**1**), *trans-2* ((±)-**2**), and *trans-3* ((±)-**3**) addition patterns on the C-sphere were prepared by *Bingel* macrocyclization. The *trans-1* derivative (±)-**1** was obtained in 30% yield, together with a small amount of (±)-**2** by cyclization of the dibenzo[18]crown-6(DB18C6)-tethered bis-malonate **4** with C_{60} (*Scheme 1*). When the crown-ether tether was further rigidified by K^+-ion complexation, the yield and selectivity were greatly enhanced, and (±)-**1** was obtained as the only regioisomer in 50% yield. The macrocyclization, starting from a mixture of tethered bis-malonates with *anti* (**4**) and *syn* (**10**) bisfunctionalized DB18C6 moieties, afforded the *trans-1* ((±)-**1**, 15%), *trans-2* ((±)-**2**, 1.5%), and *trans-3* ((±)-**3**, 20%) isomers (*Scheme 2*). Variable-temperature ^{1}H-NMR (VT-NMR) studies showed that the DB18C6 moiety in C_2-symmetrical (±)-**1** cannot rotate around the two arms fixing it to the C-sphere, even at 393 K. The planar chirality of (±)-**1** was confirmed in ^{1}H-NMR experiments using the potassium salts of (*S*)-1,1′-binaphthalene-2,2′-diyl phosphate ((+)-(*S*)-**19**) or (+)-(1*S*)-camphor-10-sulfonic acid ((+)-**20**) as chiral shift reagents (*Fig. 1*). The DB18C6 tether in (±)-**1** is a true covalent template: it is readily removed by hydrolysis or transesterification, which opens up new perspectives for molecular scaffolding using *trans-1* fullerene derivatives. Characterization of the products **11** (*Scheme 3*) and **18** (*Scheme 4*) obtained by tether removal unambiguously confirmed the *trans-1* addition pattern and the *out-out* geometry of (±)-**1**. VT-NMR Studies established that (±)-**2** is a C_2-symmetrical *out-out trans-2* and (±)-**3** a C_1-symmetrical *in-out trans-3* isomer. Upon changing from (±)-**1** to (±)-**3**, the distance between the DB18C6 moiety and the fullerene surface increases and, correspondingly, rotation of the ionophore becomes increasingly facile. The ionophoric properties of (±)-**1** were investigated with an ion-selective electrode membrane (*Fig. 2* and *Table 2*), and K^+ was found to form the most stable complex among the alkali-metal ions. The complex between (±)-**1** and KPF_6 was characterized by X-ray crystal-structure analysis (*Figs. 3* and *4*), which confirmed the close tangential orientation of the ionophore atop the fullerene surface. Addition of KPF_6 to a solution of (±)-**1** resulted in a large anodic shift (90 mV) of the first fullerene-centered reduction process, which is attributed to the electrostatic effect of the K^+ ion bound in close proximity to the C-sphere (*Fig. 5*). Smaller anodic shifts were measured for the KPF_6 complexes of (±)-**2** (50 mV) and (±)-**3** (40 mV), in which the distance between ionophore and fullerene surface is increased (*Table 3*). The effects of different alkali- and alkaline-earth-metal ion salts on the redox properties of (±)-**1** were investigated (*Table 4*). These are the first-ever observed effects of cation complexation on the redox properties of the C-sphere in fullerene-crown ether conjugates.

1. Introduction. – With the development of the covalent chemistry of buckminsterfullerene C_{60} [1], an increasing number of covalent fullerene-crown-ether conjugates have been prepared (for reviews on supramolecular fullerene chemistry,

[1]) Fax: +41-1-6321109; e-mail: diederich@org.chem.ethz.ch.

see [2])[3]. Targets of these research efforts were the formation of amphiphilic fullerene derivatives which undergo *Langmuir* monolayer formation at the air-water interface [4], and the formation of supramolecular complexes [5] and assemblies [6] by metal or ammonium ion recognition. In the complexation studies, it was expected that cation binding would affect the redox potential of the fullerene sphere, thereby providing an electrochemically detectable sensoric signal for the recognition event (for a review on fullerene electrochemistry, see [7]). However, due to large distances between the ionophore-bound cation and the C-sphere, no influence of cation complexation on the redox properties of the latter was measured for the early fullerene-crown ether conjugates.

It became clear from these studies that a significant, electrochemically detectable perturbation of the electronic structure of C_{60} could be expected only if the ionophore-bound metal ion is positioned closely and tightly atop the fullerene surface. Therefore, we became interested in rigorously controlling the distance and orientation between crown ether and C-sphere by attaching the ionophore to two points of the C_{60} surface, leading to the formation of a cyclophane structure. Experimentally, this is best achieved by *Bingel* macrocyclization [8] (for a review on tether-directed remote functionalization methods, see [9]), the efficient regio- and stereoselective cyclization of C_{60} with tethered bis-malonates in a double *Bingel* addition [10]. This reaction provides a highly effective method for precisely positioning organic chromophores in close proximity to the fullerene surface (for recent examples, see [11]).

Here, we report the synthesis of the fullerene-crown ether conjugates (±)-**1** to (±)-**3** with *trans-1* ((±)-**1**), *trans-2* ((±)-**2**), and *trans-3* ((±)-**3**) addition patterns on the C-sphere (for the position notation of the bis-adducts, see [12]) by *Bingel* macrocyclization. We provide evidence for a remarkable template effect of K^+ ions on the cyclization leading to (±)-**1**. Whereas this tether-directed remote-functionalization methodology had previously been applied to prepare bis-adducts with *cis-2*, *cis-3*, *e*, *trans-4*, and *trans-3* addition patterns [8][9], regioselective access to *trans-2* and *trans-1* derivatives by this route had proven difficult prior to this work (for a preliminary communication of parts of this work, see [13]), mainly due to the challenge to design extended tethers with a suitable degree of conformational homogeneity that would span the entire fullerene sphere (for regioselective access to *trans-1* bis-adducts, see [11a]; for *trans-2* bis-adducts, see [11b])[14]. We show that the dibenzo[18]crown-6 (DB18C6) tether in (±)-**1** is a true template that can be readily removed, thereby providing a versatile entry into diverse fullerene molecular scaffolding. The ionophoric properties of (±)-**1** are determined with an ion-selective electrode membrane, and the X-ray crystal structure of the 1:1 complex formed between (±)-**1** and KPF_6 is described. We also demonstrate in extensive electrochemical studies with (±)-**1** to (±)-**3** that, for the first time, cation complexation strongly affects the redox potentials of C_{60} as a result of the close proximity of the ionophore-bound cation to the fullerene surface.

2. Results and Discussion. – 2.1. *Synthesis of the Fullerene-Crown Ether Conjugates.* For the *Bingel* macrocyclization, bis-malonate **4** with the DB18C6 tether had been designed with the help of molecular modeling to ensure a tangential orientation of the crown ether atop of the fullerene sphere [15]. Semi-empirical PM3 calculations [16] predicted that the relative stability of the three regioisomers, which would preferen-

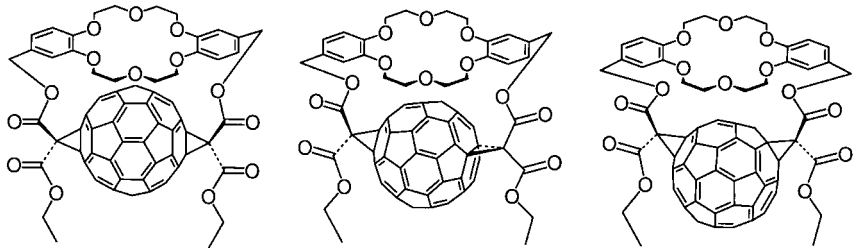

(±)-**1**
(*trans-1*)

(±)-**2**
(*trans-2*)

(±)-**3**
(*trans-3*)

tially form by addition of **4** to C_{60}, would be in the order *trans-1* > *trans-2* > *trans-3*. We, therefore, expected a preferential formation of (±)-**1**, if product stability is reflected in the transition state of the second cyclopropanation step of the macrocyclization.

In the synthesis of **4** (*Scheme 1*), 3,4-dihydroxybenzaldehyde was regioselectively alkylated with an excess of bis(2-chloroethyl) ether to give **5** as colorless needles [17]. The two minor side-products, the regioisomer of **5** formed by alkylation of the OH group at C(3) (a yellow oil) and the compound resulting from linking two 3,4-dihydroxybenzaldehyde molecules, could be readily separated. Macrocyclization of **5**, templated by K^+ ions [18], yielded dialdehyde **6**, which was reduced to diol **7** and subsequently transformed into bis-malonate **4**. A modified *Bingel* reaction [8] of **4** with C_{60} in PhMe yielded the *trans-1* derivative (±)-**1** as the major product in 30% yield together with a minor amount of *trans-2* derivative (±)-**2** (3%), in agreement with the computational predictions. This regioselectivity could be strongly increased by addition of KPF_6 while performing the macrocyclization in PhMe/MeCN 96 : 4 to increase the solubility of the salt. Under these conditions, (±)-**1** was formed as the unique regioisomer in 50% yield! The remarkable improvement both in yield and regioselectivity of the macrocyclization is undoubtedly due to the templating effect of the K^+

Scheme 1. *Synthesis of (±)-**1***

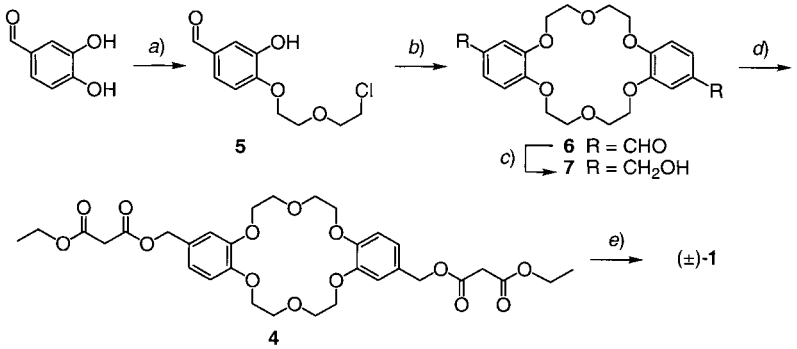

a) $Cl(CH_2)_2O(CH_2)_2Cl$, K_2CO_3, DMF, 80°, 36 h; 23%. *b*) K_2CO_3, DMF, 80°, 24 h; 47%. *c*) $NaBH_4$, MeOH, r.t., 1 h; 72%. *d*) $ClCOCH_2CO_2Et$, pyridine, CH_2Cl_2, r.t., 1 h; 69%. *e*) C_{60}, I_2, 1,8-diazabicyclo[5.4.0]undec-7-ene (DBU), KPF_6, PhMe/MeCN, r.t., 6 h; 50%.

ion [19], which binds to the DB18C6 moiety in **4** (see below) [20], making the tether more rigid and, thereby, more selective, enhancing the preference of the second cyclopropanation to occur in the *trans-1* position.

When DB18C6 was diformylated by the *Smith* modification [21] of the *Duff* reaction [22], a 1:1 mixture of *anti* and *syn* isomers **6** and **8** was obtained (*Scheme 2*) [23]. Their reduction to **7** and **9**, respectively, conversion to the bis-malonates **4** and **10**, and treatment of the mixture under modified *Bingel*-reaction conditions afforded the *trans-1* ((±)-**1**, 15%), *trans-2* ((±)-**2**, 1.5%), and *trans-3*, ((±)-**3**, 20%) isomers, which were separated by flash chromatography on SiO_2-*H* (AcOEt/PhMe 1:1). Thus, conversion of the *syn* isomer **10**, with the smaller extension of its tether, provided regioselectively the *trans-3* derivative (±)-**3**.

Scheme 2. *Synthesis of (±)-***2** *and (±)-***3**

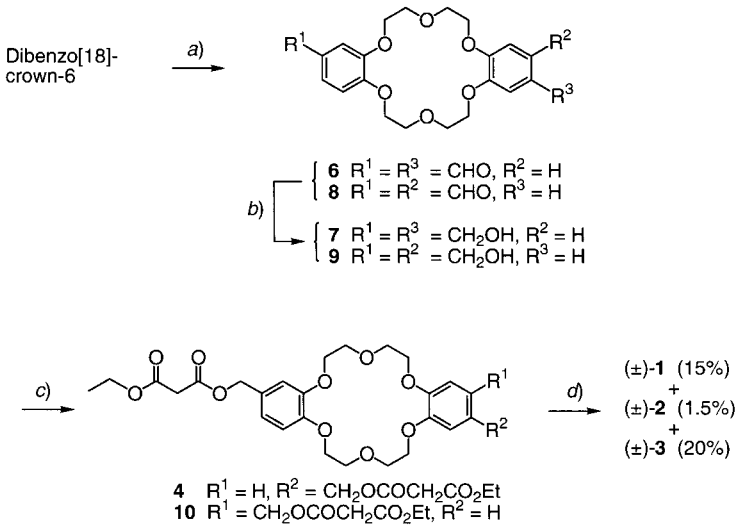

a) Hexamethylenetetramine ($(CH_2)_6N_4$), CF_3COOH, 115°, 24 h; 21%. *b*) $NaBH_4$, $CHCl_3$, r.t., 36 h; 52%. *c*) $ClCOCH_2CO_2Et$, Et_3N, DMF, r.t., 2 h; 74%. *d*) C_{60}, I_2, DBU, PhMe, r.t., 14 h.

2.2. *Structural Assignment and Chemical Reactivity of the Fullerene-Crown Ether Conjugates.* The relative position of the two cyclopropane rings on the C_{60} surface in the three fullerene-crown ether conjugates was established by ^{1}H-NMR, ^{13}C-NMR, and UV/VIS spectroscopy. In particular, the crown-ether tethers do not perturb the UV/VIS absorption of the C-spheres above 300 nm, and the spectra of the three isomers correspond to those previously reported for *trans-1*, *trans-2*, and *trans-3* bis(diethyl malonate) adducts [8][24][25]. The ^{1}H- and ^{13}C-NMR spectra support the C_2 symmetry of (±)-**1** and (±)-**2**, and the C_1 symmetry of (±)-**3**.

2.2.1. trans-1 *Conjugate (±)-***1**. The addition pattern of (±)-**1** was confirmed by transesterification with removal of the tether (*Scheme 3*). Thus, the reaction of (±)-**1** with Cs_2CO_3 in anhydrous hexanol/THF 1:1 provided the D_{2h}-symmetrical bis-adduct **11** in 34% yield. Its ^{13}C-NMR spectrum displayed only nine resonances for the fullerene C-atoms and the expected peaks for four equivalent hexyl residues. Of all possible

regioisomeric bis(dihexyl malonate) adducts of C_{60}, only the *trans-1* compound displays this high symmetry [12]. Compound **11** was also obtained by a second route. We prepared the bis(*tert*-butyl ester) (±)-**12** by transforming the DB18C6-diol **7** into bis-malonate **13**, followed by macrocyclization with C_{60}, hoping for the opportunity either to selectively remove the tether in (±)-**12** or to hydrolyze the *tert*-butyl-ester groups. These plans have failed so far since, upon heating with TsOH in PhMe, compound (±)-**12** was readily transformed into the tetracarboxylic acid **14**. Apparently, acidic cleavage of the tethered ester groups is quite favorable due to the stabilization of the intermediately formed benzylic carbocations by the *p*-alkoxy groups. The highly insoluble tetracarboxylic acid **14** was not isolated but, rather, directly transformed with oxalyl chloride into the intermediate tetrakis(acyl halide) **15** which then reacted with hexanol in the presence of pyridine to give **11** in 45% yield (starting from (±)-**12**). As a major side-product, the corresponding tris-ester (one $C_6H_{13}OCO$ residue in **11** is replaced by a H-atom) was isolated in 20% yield, which presumably results from monodecarboxylation during the hydrolysis of (±)-**12** and subsequent esterification *via* the tris(acyl halide).

Scheme 3. *Preparation of* **11** *by Transesterification*

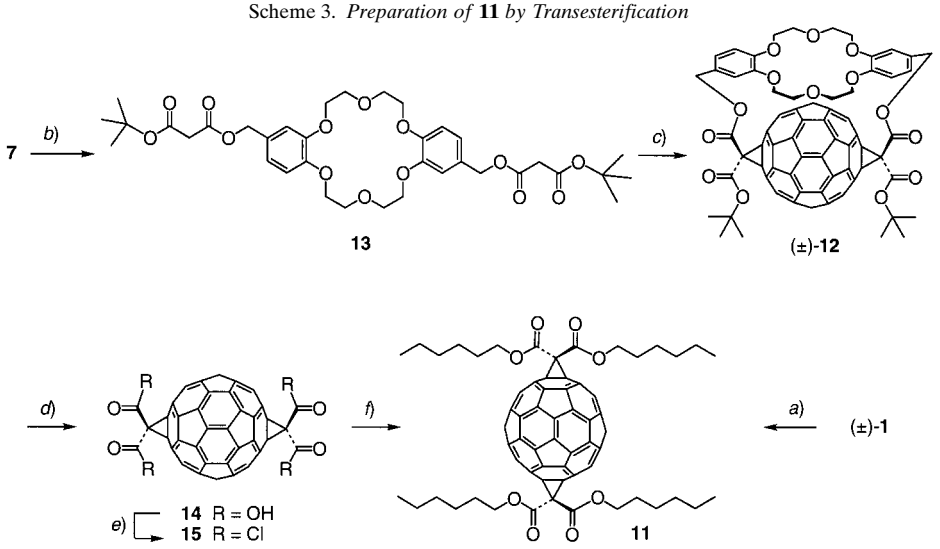

a) Hexanol/THF 1:1, Cs_2CO_3, KPF_6, r.t., 3.5 h; 34%. *b*) $ClCOCH_2CO_2$(*t*-Bu), pyridine, CH_2Cl_2, r.t., 1 h; 52%. *c*) C_{60}, I_2, DBU, KPF_6, PhMe/MeCN, r.t., 1 h; 54%. *d*) $TsOH \cdot H_2O$, PhMe, Δ, 12 h. *e*) $(COCl)_2$, CH_2Cl_2, 40°. 4 h. *f*) Hexanol, pyridine, CH_2Cl_2, r.t., 14 h; 45% (from (±)-**12**).

While the strategy to use the DB18C6 tether and the *t*-Bu groups as orthogonal ester-protecting groups failed, the facile cleavage of the crown-ether tether under acidic conditions opened up the opportunity to selectively remove this covalent template [19a] in bis(ethyl ester) (±)-**1**. This was indeed readily accomplished by heating (±)-**1** in PhMe in the presence of TsOH (*Scheme 4*). The formed dicarboxylic acid **16** was neither isolated nor purified due to its insolubility; furthermore, the compound seems to be quite sensitive to decarboxylation in the presence of even catalytic amounts of a weak base. Activation with oxalyl chloride followed by addition of triethyleneglycol

monomethyl ether to the intermediate bis(acyl halide) **17** afforded the C_{2v}-symmetrical tetraester **18** in 60–70% yield (starting from (±)-**1**). Methods to cleave the ethyl-ester residues in (±)-**1**, while keeping the crown-ether tether intact, are still under investigation. The selective transesterification of (±)-**1** to give C_{2v}-symmetrical **18** demonstrated unambiguously the *out-out* geometry of (±)-**1** [8][2]). Indeed, if the DB18C6 tether were attached in an *in-out* geometry, the corresponding transesterified compound should have C_{2h} symmetry. Later, the *out-out* geometry of (±)-**1** was also confirmed by X-ray crystal-structure analysis (see below).

Scheme 4. *Synthesis of* **18** *by Selective Removal of the DB18C6 Tether*

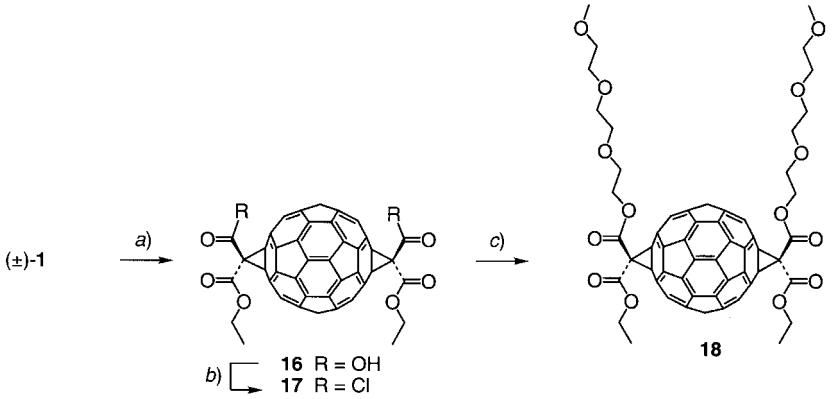

a) $TsOH \cdot H_2O$, PhMe, Δ, 3 h. *b*) $(COCl)_2$, CH_2Cl_2, 40°, 2 h. *c*) triethyleneglycol monomethyl ether, pyridine, CH_2Cl_2, r.t., 14 h; 68% (from (±)-**1**).

The above transesterification protocols clearly established that the DB18C6 tether is a true template, which can be readily removed after accomplishing the task to direct the addition into the *trans-1* position. This opens up a versatile entry into diverse molecular scaffolding using *trans-1* functionalized fullerenes.

The planar chirality of C_2-symmetrical (±)-**1** was established with the help of two chiral shift reagents. Upon addition of 1 equiv. of the potassium salts of (*S*)-1,1′-binaphthalene-2,2-diyl phosphate ((+)-(*S*)-**19**) or (+)-(1*S*)-camphor-10-sulfonic acid ((+)-**20**) to (±)-**1** ($c = 2.5$ mM) in $CDCl_3$, a doubling of several resonances of the DB18C6 moiety of (±)-**1** was detected in the ^{1}H-NMR spectrum (*Fig. 1*). It is reasonable to assume that the crown-ether moiety of (±)-**1** binds these potassium salts as tight ion pairs (see below), and that the optically active counteranions differentially shift the resonances of the tether in the two formed diastereoisomeric complexes with different geometries. There is a significant barrier to rotation of the crown ether in (±)-**1**, and its enantiomers are expected to be stable toward racemization at room temperature. The ^{1}H-NMR spectrum of (±)-**1** does not change significantly upon heating a solution in $(CDCl_2)_2$ from 298 to 393 K: the characteristic *AB* system for the

---

[2]) In theory, each of the three fullerene-crown ether conjugates (±)-**1**–(±)-**3** could be formed as a mixture of configurational diastereoisomers, depending on how the ethoxycarbonyl residues at the two methano-bridge C-atoms are oriented with respect to each other (*in-in*, *in-out*, and *out-out* stereoisomerism).

benzylic CH_2 protons in the tether is maintained at the high temperature, and no indication for coalescence is observed. If rotation would be fast at higher temperature, the benzylic CH_2 protons of the tether would feature a *singlet*.

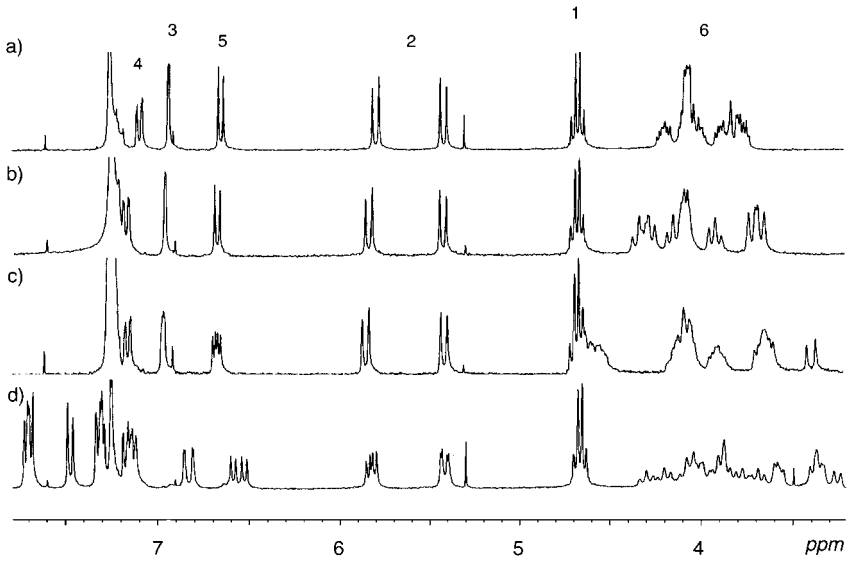

Fig. 1. *^{1}H-NMR Spectra* ($CDCl_3$, 300 MHz) *of pure (±)*-**1** ($c = 2.5$ mM) (a) *and in the presence of 1 equiv. of* KPF_6 (b), *(+)*-**20** (c), *and (+)-(*S*)*-**19** (d). Arbitrary numbering is shown for (±)-**1**.

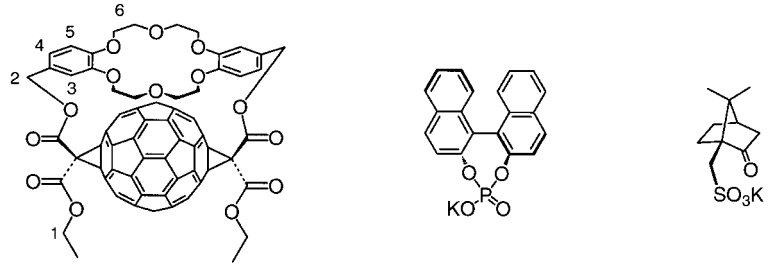

(±)-**1** (+)-(*S*)-**19** (+)-**20**

2.2.2. trans-2 *Conjugate (±)*-**2**. This crown-ether conjugate can theoretically exist in three configurationally diastereoisomeric forms, namely C_2-symmetrical *in-in* or *out-out*, and C_1-symmetrical *in-out* [8]. The ^{1}H-NMR spectrum (500 MHz, $(CDCl_2)_2$) of (±)-**2** at 392 K showed the presence of one C_2-symmetrical molecule; for example, one *AB* system was measured for the benzylic CH_2 protons. Correspondingly, the ^{13}C-NMR spectrum (125 MHz, $CDCl_3$) at 293 K displayed the 28 resonances expected for the sp^2-C-atoms of the C_{60} sphere in a C_2-symmetrical derivative. Computer simulations with the MM2 force field [26] indicated that the *in-in* isomer can only adopt much less favorable conformations than the *out-out* isomer. The most favorable *in-in* geometries, with the DB18C6 in a tangential orientation to the fullerene surface, are by more than 30 kcal mol^{-1} higher in steric energy than the best *out-out* ones; we, therefore, assign

with confidence the depicted *out-out* structure to the *trans-2* derivative (±)-**2**. Variable-temperature ^{1}H-NMR (VT-NMR) spectra revealed that, at 392 K, rapid equilibration between two C_2-symmetrical diastereoisomeric conformers occurs, with the DB18C6 moiety rotating fast around the two arms fixing it to the C-sphere[3]). This shows that the distance between ionophore and fullerene surface is significantly larger in the *trans-2* derivative (±)-**2** than in the *trans-1* derivative (±)-**1** since, in the latter, the same crown-ether moiety was unable to rotate on the ^{1}H-NMR time scale even at 393 K (*Sect. 2.2.1*). Below *ca.* 333 K, the rotation of the DB18C6 moiety becomes slow on the ^{1}H-NMR time scale, and two sets of resonances with an intensity ratio of *ca.* 10 : 3 appear, indicating slow exchange between two differently populated diastereoisomeric conformers. According to a lineshape-fitting procedure [27], the activation parameters for the rotation of the crown-ether moiety in (±)-**2** in $CDCl_3$ were determined. The iteratively fitted lineshape was calculated on the basis of a simple two-site exchange mechanism [28]. The rate constant k and the activation free enthalpy $\Delta G^{\neq}$ (*Table 1*) were determined for six temperatures in the interval between 243 and 298 K by comparison of the global shape of the experimental spectrum with the simulated one. At 298 K, $\Delta G^{\neq}$ for the rotation of the crown ether moiety in (±)-**2** is 19 kcal mol^{-1}. The activation parameters $\Delta H^{\neq}$ and $\Delta S^{\neq}$ (*Table 1*) were determined from an *Eyring* plot *via* linear-regression analysis.

Table 1. *Activation Parameters from VT-NMR Experiments* (500 MHz, $CDCl_3$) *for the Rotation of the Crown Ether in (±)-***2**

Proton[a])	δ [ppm]	$\Delta G^{\neq}_{298\,K}$ [kcal mol^{-1}]	$\Delta H^{\neq}$ [kcal mol^{-1}]	$\Delta S^{\neq}$ [cal grad^{-1} mol^{-1}]
H–C(2)	5.51	19 ± 1	10 ± 1	−30 ± 1
H–C(5)	6.57	19 ± 2	9 ± 1	−32 ± 4
H–C(4)	7.11	19 ± 1	9 ± 1	−33 ± 2

[a]) The arbitrary C-atom numbering is the same as shown in *Fig. 1* for (±)-**1**.

2.2.3. trans-3 *Conjugate (±)*-**3**. The *trans-3* isomer with the *syn*-bisfunctionalized DB18C6 tether can, in theory, also exist in three configurationally diastereoisomeric forms, C_2-symmetrical *in-in* and *out-out* and C_1-symmetrical *in-out*, provided the rotation of the crown ether around its two arms linking it to the C-sphere is fast. If, however, this rotation is slow, and the crown ether adopts one stable conformation tangential to the fullerene surface, the symmetry in all three configurational diastereoisomers is reduced to C_1. The ^{1}H-NMR spectrum (500 MHz, $(CDCl_2)_2$) of (±)-**3** at 333 K clearly showed the presence of one C_1-symmetrical isomer; for example, one *AB* system and one *singlet* appear in the ^{1}H-NMR spectrum for the two benzylic CH_2 groups. Also, the ^{13}C-NMR spectrum (125 MHz, $(CDCl_2)_2$) at 333 K depicts 50 (of 56 expected) resonances for the sp^2-C-atoms of the C-sphere. VT-NMR Measurements provided clear evidence that the spectra at 333 K reflected the presence of the *in-out trans-3* diastereoisomer (with a rapidly rotating crown ether) rather than the preferred population of one conformer of any of the three configurational diastereoisomers (at slow rotation of the DB18C6 moiety). The spectrum obtained at 243 K showed a

[3]) At rapid rotation, the observed C_2 symmetry of the entire molecule results from the C_2-symmetrical *trans-2* addition pattern of the fullerene.

doubling of the two *AB* systems for the benzylic CH_2 protons and of some of the aromatic resonances, which is consistent with the existence of two slowly equilibrating conformers at that temperature. A lineshape analysis for the determination of the activation parameters was complicated by the rotation of the *syn*-bisfunctionalized DB18C6 around its two arms, which can occur in two different directions. As a consequence of these two mechanisms of rotation, which seem to have similar activation barriers, it was not possible to simulate the lineshape evolution through the entire temperature window from 243 to 313 K. Furthermore, the activation parameters obtained for different protons varied significantly. Precise values were not obtained, but the lower limit for the activation free enthalpy for rotation of the DB18C6 moiety in (±)-**3** can be estimated as $\Delta G^{\ddagger}_{298\,K} \approx 14$ kcal mol^{-1}.

2.3. *Ionophoric Properties of the* trans-1 *Fullerene-Crown Ether Conjugate (±)*-**1**. The ionophoric properties of (±)-**1** were investigated using a solvent-polymeric ion-selective electrode (ISE) membrane containing the fullerene-crown ether conjugate, sodium tetrakis[3,5-bis(trifluoromethyl)phenyl]borate (NaTFPB), bis(2-ethylhexyl) sebacate (DOS), and high-molecular-weight poly(vinyl chloride) (PVC) [29][30]. A close to theoretical (*Nernstian*) potentiometric response was found for all monovalent ions investigated (*Fig. 2*) which allows the potentiometric selectivity coefficients, $\log K^{pot}_{K,J}$, to be correctly determined by the separate solution method (*Table 2*, *Column 2*) [31][32]. Since this does not hold for divalent ions, only limiting values can be given in these cases. The logarithmic selectivity sequence determined this way is with J = Rb^+: -0.7 ± 0.2, NH_4^+: -0.9 ± 0.2, Na^+: -1.7 ± 0.2, Cs^+: -2.3 ± 0.4, H^+: -2.4 ± 0.3, Li^+: -2.7 ± 0.3, Mg^{2+}: < -3.5, Ca^{2+}: < -4.0, Sr^{2+}: < -4.3. This sequence clearly deviates from that of an ion-exchanger-based membrane (*Hofmeister* series [29]) and thus proves that (±)-**1** acts as an ionophore. Effective complex-formation constants, K^{eff}_{IL} (I = alkali metal ion, L = ligand), in the same solvent-polymeric phase were obtained by comparing the responses of two membranes, one with the H^+-selective ionophore ETH 2439 and NaTFPB (*Table 2*, *Column 4*) and the other additionally with (±)-**1** (*Table 2*, *Column 5*) [33]. The $\log K^{eff}_{IL}$ values (*Table 2*, *Column 6*) were calculated under the assumption of 1 : 1 stoichiometry for all alkali-metal cation-ligand complexes as 5.4 ± 0.2 (K^+), 4.0 ± 0.2 (Na^+), 3.3 ± 0.5 (Cs^+), and 2.9 ± 0.3 (Li^+). For K^+, Na^+, and Li^+, they are lower by 3.9, 2.7, and 3.8 orders of magnitude, respectively, than for valinomycin as ligand in the same membrane matrix [33][34].

2.4. *X-Ray Crystal Structure of* trans-1 *Conjugate (±)*-**1**. Black, plate-like single crystals of (±)-**1** were obtained by slow evaporation of a solution of CH_2Cl_2/PhH at room temperature. The crystals belong to the monoclinic space group *C*2/*c*, and the X-ray structure was determined at 243 K. Further details about the X-ray analysis are given in the *Exper. Part.*

The crystal structure of (±)-**1**, viewed from two different perspectives, is shown in *Figs. 3* and *4*. The numbering of the C_{60} skeleton used (*Fig. 3*) follows that proposed by *Taylor* [35]. Substantial disorder is observed: one of the ethyl-malonate moieties (C(92) to C(101)), the PF_6^- anion, and the two included solvent molecules (CH_2Cl_2 and benzene; not shown) are disordered. For C(92), O(93), O(95), O(99), C(100), and C(101) of the malonate and the F-atoms of the counteranion, the disorder could be resolved, *i.e.*, two sets of atomic parameters were refined, leading to two different

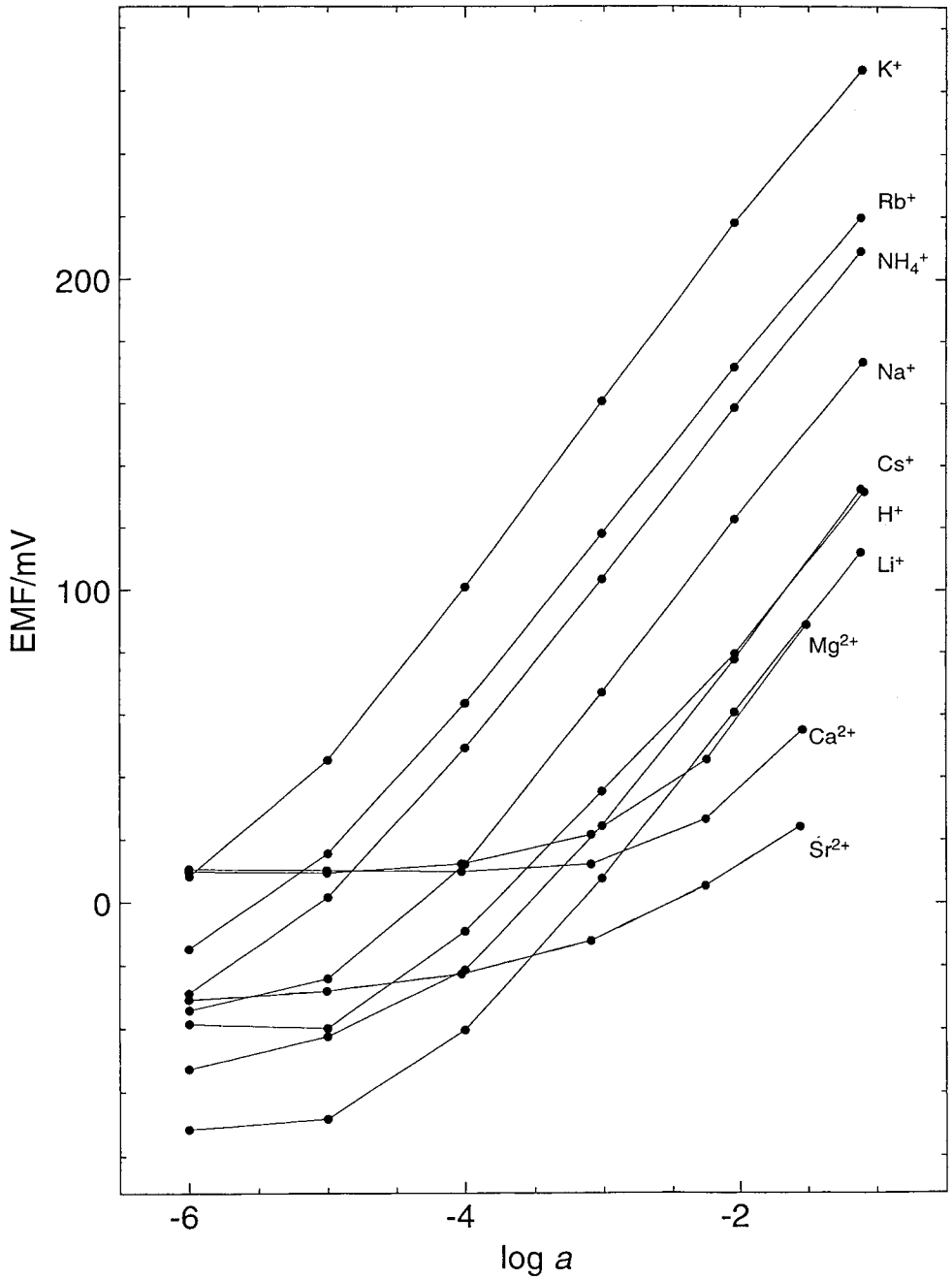

Fig. 2. *Response of a (±)-***1***-based ISE membrane* (DOS/PVC) *to* K^+ *and various interfering ions.* EMF = electromotive force. a = activity.

Table 2. *Potentiometric Selectivity Coefficients, log* K_{IJ}^{pot}, *of ISE Membranes* (DOS/PVC) *Based on* (±)-**1**, *ETH 2439, or Both, and Effective Complex-Formation Constants, log* K_{IL}^{eff}, *of* (±)-**1** *in the Membrane with Various Cations* (J)[a]

J	log K_{IJ}^{pot} for I				log K_{IL}^{eff}
	K^+		H^+		
	(±)-**1**[b])[c])	(±)-**1**[c])	ETH 2439[c])	(±)-**1**/ETH 2439[c])	
H^+	−2.4±0.3	0	0	0	
Li^+	−2.7±0.3	−0.3±0.4	−7.9±0.3	−7.2±0.3	2.9±0.3
Na^+	−1.7±0.2	0.7±0.4	−7.7±0.2	−6.2±0.2	4.0±0.2
K^+	0	2.4±0.3	−7.3±0.1	±4.5±0.4	5.4±0.2
Cs^+	−2.3±0.4	0.1±0.5	−6.9±0.2	−6.0±0.3	3.3±0.5

[a]) Standard deviations from measurements with three ISEs from the same membrane. [b]) log $K_{K,J}^{pot}$ for J = Rb^+: −0.7±0.2, NH_4^+: −0.9±0.2, Mg^{2+}: <−3.5, Ca^{2+}: <−4.0, Sr^{2+}: <−4.3. [c]) Membranes based on ionophore (±)-**1** (L) and/or chromoionophore ETH 2439.

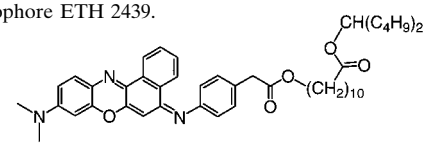

ETH 2439

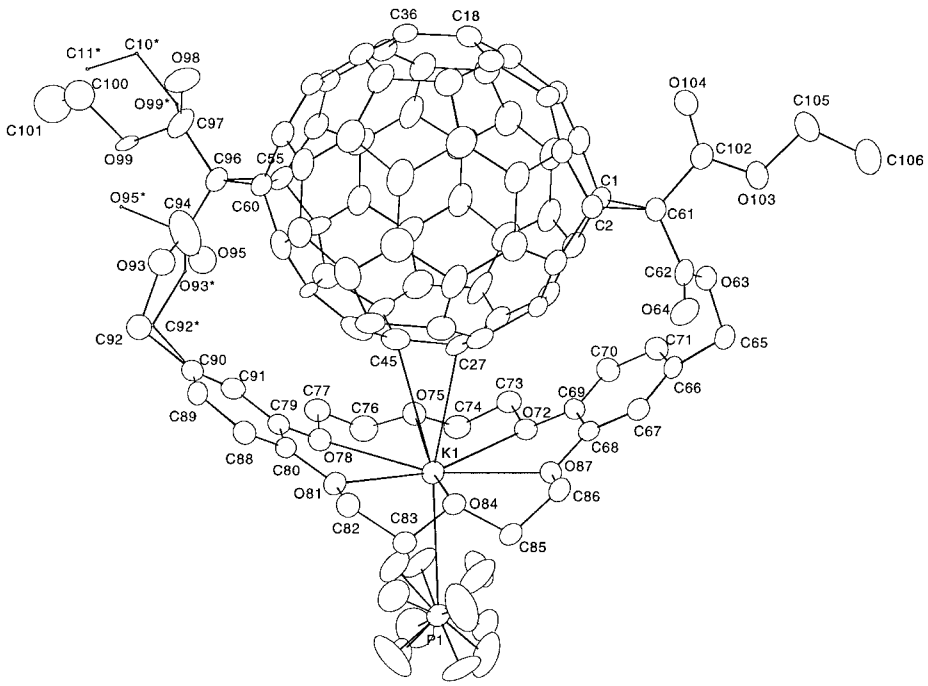

Fig. 3. *X-Ray crystal structure of* (±)-**1**. Atomic displacement parameters obtained at 243 K are drawn at the 20% probability level, except for starred (*) atoms of orientation 2 of the disordered ethyl-malonate moiety, which are reduced for clarity.

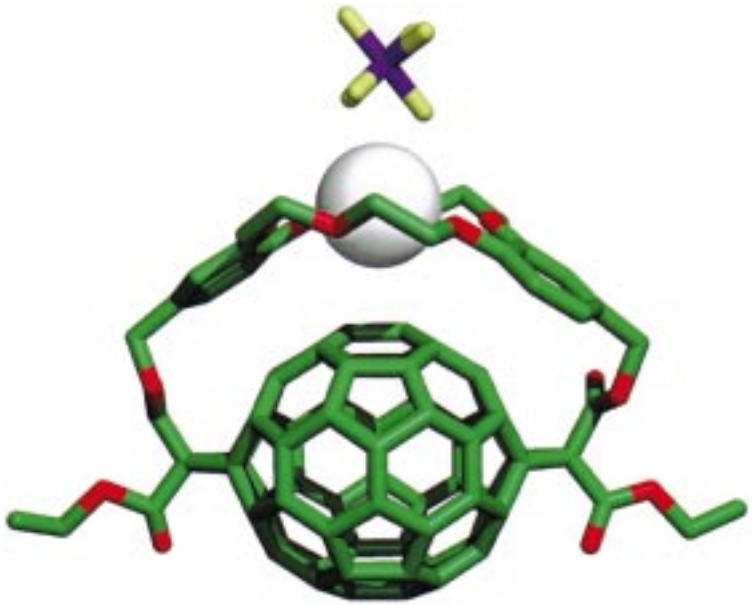

Fig. 4. *Graphical visualization of the X-ray crystal structure of (±)-***1**

orientations of the corresponding sub-units. Within the ordered part of the structure, the estimated standard deviations (e.s.d.'s) range from *ca.* 0.01 to 0.015 Å for bond lengths and from *ca.* 0.5 to 1° for bond angles. Within the disordered part of the structure, the observed geometry is much less reliable than the corresponding e.s.d.'s could suggest.

The X-ray crystal structure of the fullerene-crown ether conjugate clearly confirms the *trans-1* addition pattern with the *out-out* geometry, which had been previously deduced on the basis of chemical transformations, and ^{1}H- and ^{13}C-NMR spectroscopic data [13]. It also shows the close tangential orientation of the ionophore moiety with respect to the fullerene surface, which had been predicted by computer modeling. The disorder observed within the ethyl-malonate sub-units suggests that the fullerene-crown ether conjugate adopts two different conformations with roughly equal probability. The nature of the disorder is not clear. Thus, we do not know whether the disordered ethyl-malonate moiety jumps from one orientation to the other during the X-ray experiment, or if there are two slightly different fullerene-crown ether conjugates at (formally) symmetry-equivalent sites within the unit cell. According to the spectral data, (±)-**1** has C_2 symmetry in solution (see *Sect. 2.2.1*). Based on the X-ray results described below, the symmetry of (±)-**1** in the crystal is C_1. *Fig. 3* indicates, however, that the molecule including the fragment C(92), O(93), C(94), O(95), C(96), C(97) to C(101) is somewhat closer to the C_2 symmetry found in solution than that including the fragment C(92*), O(93*), C(94), O(95*), C(96), C(97) to C(11*).

The ordered C_{60} skeleton has a pseudo-ellipsoidal shape with principal axes of *ca.* 7.36, 6.94, and 6.83 Å, the longest being the distance between the fusion bonds C(1)–C(2) and C(55)–C(60), and the shortest between the 6-6 bonds C(18)–C(36) and C(27)–C(45).

The DB18C6 moiety has a similar shape to that found in the X-ray crystal structure of the complexes formed between DB18C6 and KPF_6 [36a], and other potassium salts [36b]. As in these complexes, the conformation of the DB18C6 moiety in (±)-**1** is characterized by antiperiplanar C–O and synclinal C–C bonds except, of course, those in the benzene rings. The six crown-ether O-atoms are approximately coplanar (within 0.19 Å), and the cation is shifted out of this plane by *ca.* 0.4 Å in the direction of the P-atom of the counteranion. This out-of-plane shift of the K^+ ion in (±)-**1** is by *ca.* 0.3 Å larger than the corresponding values reported for three independent $DB18C6 \cdot KPF_6$ complexes [36a], in which the potassium ion bound crown ether is 'sandwiched' between two PF_6^- anions. Also, the six $K^+ \cdots O$ distances (2.70 to 2.87 Å, mean 2.79 Å) in (±)-**1** are, on average, *ca.* 0.03 Å longer than the corresponding distances reported in [36a]; furthermore, the dihedral angle between the planes of the two aromatic rings (107°) is reduced by *ca.* 21°, 13°, and 9°, respectively, as compared to the three reported $DB18C6 \cdot KPF_6$ structures [36a]. The observed differences must be related partially to the nature of counteranion coordination: in (±)-**1**, the K^+ ion is coordinated to only one counteranion, whereas in the three $DB18C6 \cdot KPF_6$ structures [36a], the cation is sandwiched between two counteranions. An evaluation of the $K^+ \cdots F$ distances in (±)-**1** is unreliable due to the disorder of the F-atoms.

Interactions between the $DB18C6 \cdot K^+$ moiety with the fullerene sphere are also observed. The shortest contacts between the ionophore and the C-sphere (C(80)⋯C(46) and C(69)⋯C(26) are *ca.* 3.23 Å. The benzene ring formed by C(79), C(80), C(88), C(89), C(90), and C(91) is in close stacking contact with the fullerene pentagon consisting of C(44), C(45), C(46), C(57), and C(58), with an interplanar angle of 8° and an inter-ring distance (center-to-center) of 3.45 Å. The second benzene ring of the ionophore is superimposed to a fullerene hexagon, with an interplanar angle of 16° and an inter-ring distance of 3.7 Å. Similar fullerene⋯aromatic ring contacts are observed in X-ray crystal structures of clathrates and solid-state complexes formed between C_{60} and extended electron-rich aromatic chromophores (for a review, see [26]; see also [37])[4]). Of interest are also the interactions between the K^+ cation and the C_{60} sphere in (±)-**1**. The ion is not sitting on the two-fold axis of the C_{60} core, but is shifted towards the center of the hexagon comprising C(25), C(26), C(27), C(43), C(44), and C(45). The shortest contacts $K^+ \cdots C(27)$ and $K^+ \cdots C(45)$ are 3.42 and 3.46 Å, respectively, and the distance of the K^+ ion to the corresponding ring center is *ca.* 3.7 Å. Similar contacts (3.33 to 3.59 Å) were observed in other X-ray crystal structures between K^+ ions and aromatic rings [39] and have been interpreted in terms of cation⋯π interactions [40].

2.5. *Electrochemical Studies.* To analyze the effect of cation complexation on the redox properties of the three fullerene-crown ether conjugates (±)-**1** to (±)-**3**, cyclic voltammetric (CV) studies were performed in degassed $MeCN/CH_2Cl_2$ 1:1 (+ 0.1M Bu_4NPF_6). First, the effect of K^+-ion complexation was investigated. The CV of (±)-**1** is shown in *Fig. 5*, both in the presence of 1 equiv. of [2.2.2]cryptand and in the presence of 10 equiv. of KPF_6. The cryptand was added to try to ensure that the species observed

---

[4]) A solid-state complex between C_{60}^- and $DB18C6 \cdot K^+$ has also been reported and its structure investigated by cross-polarization magic-angle-spinning ^{13}C-NMR spectroscopy (see [38]).

initially was uncomplexed[5]). The first, fullerene-based reduction process of uncomplexed (±)-**1** is quasi-reversible ($\delta E_{pp} = 70$ mV) and occurs at $E_{1/2} = -1.04$ V *vs.* the internally added ferrocene/ferricinium (Fc/Fc^+) couple (*Table 3*). The second, fullerene-based reduction process is somewhat more complicated and exhibits what appears to be two closely-spaced waves. Because of these observations, we did not

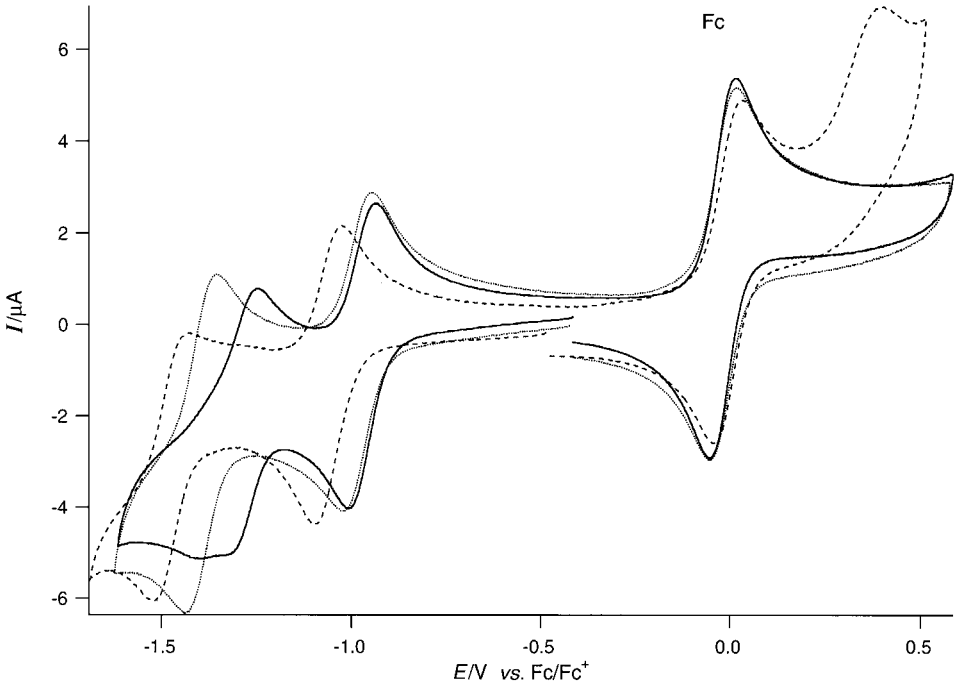

Fig. 5. *Cyclic voltammograms for (±)-***1** *recorded at 100 mV* s^{-1} *on a glassy carbon electrode in the presence of* a) *1 equiv. of [2.2.2]cryptand* (- - - -), b) *10 equiv. of* KPF_6 (⋯), *and* c) *10 equiv. of* $Ba(CF_3SO_3)_2$ (——). Fc = internally added ferrocene.

Table 3. *Redox Potentials for Compounds (±)-***1**, *(±)-***2**, *(±)-***3**, *and* **11** (0.5 mM) *in MeCN/*CH_2Cl_2 *1 : 1* (+ 0.1M Bu_4NPF_6). Potentials were referenced to internal Fc/Fc^+ and measured on a glassy carbon working mini-electrode. Values are reported in the presence of [2.2.2]cryptand (1 equiv.) and in the presence of a tenfold excess of KPF_6. Values in parentheses are the ΔE_{pp} in mV

	+ [2.2.2]cryptand		+ KPF_6	
	$E^1_{1/2}$	$E^2_{1/2}$	$E^1_{1/2}$	$E^2_{1/2}$
(±)**1**	−1.04 (70)	−1.51[a])	−0.95 (79)	−1.36 (104)
(±)**2**	−1.02 (79)	−1.48[a])	−0.97 (75)	−1.43[a])
(±)-**3**	−1.05 (83)	−1.47[a])	−1.01 (77)	−1.46[a])
11	−0.94 (77)	−1.36 (80)	−0.95 (85)	−1.36 (93)

[a]) Cathodic peak potential.

[5]) Peaks corresponding to the Na^+ and K^+ complexes were observed in the FAB mass spectrum of free (±)-**1**; these associations presumably form under the conditions of the mass-spectrometry experiments.

attempt to quantify $E_{1/2}$ for this process. The chemically irreversible oxidation observed around $+0.4$ V corresponds to the added cryptand.

Addition of substoichiometric amounts of KPF_6 to the solution of (±)-**1** resulted in the clear appearance of two new redox processes which are anodically shifted relative to those of the free conjugate. When the stoichiometric ratio is exactly 0.5, two very close, yet clearly discernible, reversible waves of approximately equal intensity are observed for the first reduction process; the original one for the parent compound at -1.04 V, which remains unshifted, and the new one, corresponding to the 1 : 1 complex, which appears at -0.95 V, anodically shifted by 90 mV. This 90-mV shift in potential, relative to that of uncomplexed (±)-**1**, is attributed to the electrostatic effect of the K^+ ion being bound in close proximity to the C-sphere. If KPF_6 is incrementally titrated into the solution containing (±)-**1**, it is possible to see the gradual decrease of the original first reduction wave and the growth of the one for the complex, exhibiting an isopotential point[6]). This behavior clearly indicates the formation of a highly stable complex between K^+ and (±)-**1** [41]. The second redox process in the complex has $\Delta E_{pp} = 100$ mV and $E_{1/2} = -1.36$ V *vs.* Fc/Fc^+. Addition of a tenfold excess of [2.2.2]cryptand reversed the voltammetric response to the original voltammogram in the absence of KPF_6, which indicates that the K^+ binding process with (±)-**1** is reversible.

Very similar results were obtained from the CV studies of compounds (±)-**2** and (±)-**3**, but the observed anodic shifts for the first redox couple upon complexation with K^+ were smaller (50 mV for (±)-**2** and 40 mV for (±)-**3**; *Table 3*). The reduction of the anodic shift from 90 mV (in (±)-**1**) to 40 mV (in (±)-**3**) can be readily explained with an increasing average distance between the cation bound to the crown ether and the fullerene surface as the addition pattern changes from *trans-1*, to *trans-2*, and to *trans-3*. This increase in distance is fully supported by computer modeling and by the results of the VT-NMR studies (*Sects. 2.1.1–2.2.3*), which showed a large decrease in the barrier of rotation of the DB18C6 moiety upon changing from *trans-1* to *trans-3*.

CV Investigations of the redox behavior of (±)-**1** in $MeCN/CH_2Cl_2$ 1 : 1 in the presence of different salts (10 equiv.) were performed under slightly different experimental conditions (*Table 4*). Whereas under the conditions used to obtain the data in *Table 3*, the mixture of the two solvents was degassed, the two solvents were now degassed separately by bubbling with Ar under ultrasound sonification. Small changes in the ratio of the two solvents, due to differences in evaporation during the degassing, led to small shifts of the waves for (±)-**1** in the presence of [2.2.2]cryptand and KPF_6 (*Tables 3* and *4*). The majority of the salts were directly added to the cell as solids. Only CsOAc was first solubilized in MeOH, then mixed with a solution of (±)-**1** in CH_2Cl_2. The solvent was subsequently evaporated and the resulting solid dried under high vacuum before the CV measurements in the usual binary solvent mixture.

Metal ions with low affinity for DB18C6 such as Li^+ (*Sect. 2.3*) showed interesting effects on the redox behavior of (±)-**1**. Addition of 1 equiv. of $LiBF_4$ to the solution of (±)-**1** resulted only in anodic shifts for the corresponding oxidation peaks of both redox processes (0/1 − and 1 − /2 −), but essentially no effect on the conjugated reduction peak potentials. It was necessary to add an excess of $LiBF_4$ to see the reduction peaks

---

[6]) An isopotential point is analogous to an isosbestic point in electronic spectroscopy.

Table 4. *Redox Potentials of (±)-***1** (0.5 mM) *in the Presence of Different Salts* (10 equiv.) *in MeCN/CH_2Cl_2 1 : 1* (+ 0.1M Bu_4NPF_6). Potentials were referenced to internal Fc/Fc^+ and measured on a glassy carbon working minielectrode

	$E^1_{1/2}$	$E^2_{1/2}$
[2.2.2]Cryptand	– 1.06 (74)	– 1.52[a])
$LiBF_4$	– 0.98 (78)	– 1.40 (92)
$NaBF_4$	– 0.97 (78)	– 1.40 (90)
KPF_6	– 0.97 (82)	– 1.38 (86)
$RbBPh_4$	– 0.99 (74)	– 1.40 (80)
CsOAc	– 1.03 (82)	– 1.46[b])
NH_4PF_6	– 1.00 (84)	– 1.48[b])
$Mg(CF_3SO_3)_2$	– 0.98 (98)	– 1.32[b])
$Ba(CF_3SO_3)_2$	– 0.97 (80)	– 1.26[b])

[a]) Cathodic peak potential. [b]) Anodic peak potential.

shift as well. The redox potentials reported in *Table 4* were recorded after addition of 10 equiv. of $LiBF_4$. This behavior reflects the enhanced binding affinity of the mono- and dianion of (±)-**1** for Li^+. The dianion of (±)-**1** is a strong metal-ion binder that competes effectively with [2.2.2]cryptand. In fact, the oxidation peak of the second reduction wave of uncomplexed (±)-**1** always shows a small shoulder (*Fig. 5*) which most probably corresponds to the oxidation of a M^+ complex, where M^+ is probably Na^+ from the glassware.

In the alkali-metal ion series, complexation of Li^+, Na^+, and K^+ leads to similar anodic shifts of the first and second reduction potentials of (±)-**1** (*Table 4*), whereas the Rb^+ and Cs^+ salts induce smaller shifts. Assuming no substantial effects of the different counteranions, interactions between crown-ether-bound cations and the adjacent C_{60} moiety are strongly dependent on the charge density of the metal ion, its state of solvation, its interactions with the local crown-ether dipoles, and the distance between the metal ion and the fullerene surface. On the basis of charge density alone, Li^+ would be expected to induce the largest anodic shift. However, its fit inside the crown ether is rather poor and binding is weak; it can be assumed that the interactions of Li^+ with the counterion and external solvation (by MeCN dipoles) reduce the proximity of this ion to the fullerene core and thus counterbalance the effects of charge density on the interaction with the C-sphere. For Na^+ and even more so for K^+, the charge density is lower, but the fit in the crown ether cavity is better. Once the cation diameter is becoming too large (Rb^+ and Cs^+) [42] to allow full penetration of the cavity, the ion remains on top, outside of the crown, and its electrostatic influence on the fullerene core is reduced. The small shift induced by ammonium ion (NH_4^+) complexation can be explained in a similar way: 'tripod' H-bonding occurs on the crown ether face opposite to the C-sphere, and the distance between cationic center and fullerene surface becomes too large for a substantial electrostatic interaction.

In the case of the divalent alkaline earth cations, larger anodic potential shifts on the first reduction step could have been anticipated on the basis of charge density alone. However, *Table 4* clearly shows that the shifts for the first reduction process are of the same magnitude as those observed for the monovalent alkali-metal ions. This is most probably due to the stronger solvation of the divalent cations, which prevents their full

penetration into the crown-ether cavity. On the other hand, this solvation is apparently overcome after the second reduction, and a pronounced effect on the second wave is observed (*Fig. 5*). The conjugated oxidation peak of the second reduction step is strongly anodically shifted, reflecting tighter binding and stronger electrostatic interactions between the divalent cation and the fullerene dianion. All electrochemical data clearly demonstrate an – expectedly – much larger interaction between crown-ether-bound cations with the negatively charged than with the neutral fullerene core.

3. Conclusions. – With the synthesis of (±)-**1**-(±)-**3**, the first fullerene-crown ether conjugates were prepared in which the ionophore moiety is positioned at a close tangential orientation to the fullerene surface. The preparations of (±)-**1** and (±)-**2** also represent the first examples of *Bingel* macrocyclizations providing C_{60} bis-adducts with the *trans-1* and *trans-2* addition patterns. The conformational homogeneity of the tether connecting the bis-malonate is crucial for the regioselectivity and yield of this reaction. When K^+ ions are bound to the DB18C6 tether in bis-malonate **4**, the *Bingel* macrocyclization with C_{60} provided the *trans-1* conjugate (±)-**1** in a remarkable yield of 50% and with complete regioselectivity. In the absence of K^+ ions, the tether is less rigid and less directing, and (±)-**1** is obtained in only 30% yield together with 3% of the *trans-2* regioisomer (±)-**2**. VT-NMR Studies showed that the DB18C6 moiety in planar-chiral C_2-symmetrical (±)-**1** cannot rotate around the two arms fixing it to the C-sphere, and enantiomers of this conjugate should be stable towards racemization at room temperature. The DB18C6 tether in (±)-**1** is a true template which can be readily removed by hydrolysis or transesterification, thereby providing versatile access to diverse molecular scaffolding involving C_{60} derivatives with *trans-1* addition pattern. By characterization of the products obtained by tether removal, the *trans-1* addition pattern and the *out-out* geometry of (±)-**1** were established unambiguously. The VT-NMR studies showed that the *trans-2* derivative (±)-**2** is a C_2-symmetrical *out-out* isomer in which the DB18C6 moiety rotates with an activation free enthalpy $\Delta G^{\ddagger}_{298\,K} \approx$ 19 kcal mol^{-1}, indicating the larger distance between ionophore and fullerene moiety as compared to (±)-**1**. In the C_1-symmetrical *in-out trans-3* isomer (±)-**3**, this distance is further extended and the DB18C6 moiety rotates with an estimated activation free enthalpy $\Delta G^{\ddagger}_{298\,K} \approx 14$ kcal mol^{-1}.

The ionophoric properties of the DB18C6 moiety in (±)-**1** were investigated with an ion-selective membrane electrode, and K^+ ions were found to bind with a small selectivity over the other alkali metal ions. The complex with KPF_6 was characterized by X-ray crystal-structure analysis which showed the close tangential orientation of the ionophore moiety with respect to the fullerene surface. The crystal-structure analysis revealed short contacts between the electron-rich aromatic rings of the DB18C6 moiety and the electron-deficient fullerene surface, as well as between the crown-ether-bound K^+ ion and the C-sphere. The close proximity between the bound cation and the fullerene surface produces a significant perturbation of the electronic structure of the C-sphere which was detected by CV. The first fullerene-centered reduction process of (±)-**1** became anodically shifted by 90 mV upon complexation of K^+, whereas smaller shifts were measured for (±)-**2** (50 mV) and (±)-**3** (40 mV) in which the distance between ionophore-bound cation and C_{60} is increased. Upon complexation of divalent alkaline-earth cations by (±)-**1**, the second fullerene-based reduction wave was affected

to a particularly large extent. These are the first reported cation-mediated effects on the electrochemical properties of fullerene. Such effects had not been detected in previous fullerene-crown ether conjugates since the distance between the ionophore and the C-sphere was too large. The study also demonstrates the power of the *Bingel* macrocyclization for positioning organic chromophores in sufficiently close, precisely defined orientation to a fullerene surface to induce profound changes in the photophysical and redox properties of the carbon allotrope. The exploitation of the cation-mediated electrochemical effects for sensoric application is now further investigated and, for this purpose, novel fullerene-ionophore conjugates with high cation selectivity are under construction.

Experimental Part

General. Reagents and solvents were purchased as reagent grade and used without further purification. C_{60} (99.5%) was purchased from *Southern Chemical Group*. CH_2Cl_2 was dried over CaH_2. All reactions were performed in standard glassware under an inert atmosphere of Ar. Evaporation and concentration were performed at water-aspirator pressure, and compounds were dried at 10^{-2} Torr. Flash chromatography (FC): SiO_2-*H*, 5–40 μm, *Fluka*, with elution at 0.2–0.4 bar; SiO_2 *60*, 0.063–0.2 mm, *Fluka*, with elution at a maximum pressure of 0.1 bar. TLC: *Alugram SIL G/UV*$_{254}$, *Macherey-Nagel*, visualization by UV light at 254 nm. M.p.: *Büchi B-540* apparatus, uncorrected. UV/VIS Spectra (λ_{max} in nm (ε[l mol^{-1} cm^{-1}])): *Varian Cary 5* spectrometer. IR Spectra [cm^{-1}]: *Perkin-Elmer 1600-FTIR*. NMR Spectra: *Bruker AM 500* and *Varian Gemini 300* or *200* at 300 K, with solvent peaks as reference. FAB-MS: *VG ZAB 2SEQ* instrument; 3-nitrobenzyl alcohol as matrix. ESI-MS: *7T-Finnigan Newstar FT/MS System*, MeOH as solvent and poly(methyl methacrylate) as the internal reference. Elemental analyses were performed by the Mikrolabor at the Laboratorium für Organische Chemie, ETH-Zürich.

4-[2-(2-Chloroethoxy)ethoxy]-3-hydroxybenzaldehyde (**5**). A mixture of 3,4-dihydroxybenzaldehyde (20.0 g, 144.8 mmol), bis(2-chloroethyl) ether (42.4 ml, 362 mmol), and powdered K_2CO_3 (325 mesh, 20 g, 144.8 mmol) in DMF (120 ml) was stirred under Ar at 80° for 36 h. The mixture was washed with H_2O and extracted with 1M NaOH. The aq. phase was acidified with 1M HCl and extracted with CH_2Cl_2. The org. layer was dried ($MgSO_4$) and the solvent evaporated *in vacuo*. FC (SiO_2; CH_2Cl_2/AcOEt 95:5) and recrystallization (CH_2Cl_2/hexane) yielded **5** (8.0 g, 23%). White needles. M.p. 75–77°. IR (KBr): 3144*m* (br.), 1672*s*, 1610*m*, 1584*m*, 1504*s*, 1449*m*, 1365*m*, 1275*s*, 1206*m*, 1126*s*, 1018*w*, 940*w*, 808*m*, 653*m*, 589*w*, 557*w*. ^{1}H-NMR (300 MHz, $CDCl_3$): 3.65–3.69 (*m*, 2 H); 3.81–3.85 (*m*, 2 H); 3.90–3.94 (*m*, 2 H); 4.28–4.32 (*m*, 2 H); 6.25 (br. *s*, 1 H); 7.01 (*d*, *J* = 8.1, 1 H); 7.41 (*dd*, *J* = 1.9, 8.1, 1 H); 7.45 (*d*, *J* = 1.9, 1 H); 9.85 (*s*, 1 H). ^{13}C-NMR (75.5 MHz, $CDCl_3$): 42.83; 69.18; 69.46; 71.56; 113.07; 115.19; 124.15; 131.68; 147.26; 151.24; 191.36. FAB-MS: 245.0 (100, *M*H$^+$). Anal. calc. for $C_{11}H_{13}ClO_4$ (244.67): C 54.00, H 5.36, O 26.16, Cl 14.49; found: C 53.95, H 5.31, O 26.05, Cl 14.21.

*6,7,9,10,17,18,20,21-Octahydrodibenzo[*b,k*][1,4,7,10,13,16]hexaoxacyclooctadecin-2,13-dicarbaldehyde* (**6**). Aldehyde **5** (3.0 g, 12.3 mmol) was added to a suspension of powdered K_2CO_3 (325 mesh, 3.4 g, 24.6 mmol) in DMF (300 ml). After stirring under Ar at 80° for 24 h, the mixture was filtered through a short plug (SiO_2; CH_2Cl_2/EtOH 9:1) and the solvent was evaporated. FC (SiO_2; $CHCl_3$/MeOH 99:1) afforded **6** (1.2 g, 47%). White powder. M.p. 214–216° ($CHCl_3$/MeOH). IR (KBr): 2948*w*, 2923*w*, 2873*w*, 1684*s*, 1612*s*, 1587*s*, 1512*s*, 1438*s*, 1267*s*, 1217*m*, 1165*m*, 1133*s*, 1052*w*, 1001*w*, 925*w*, 866*w*, 832*w*, 807*w*, 747*w*, 654*w*. ^{1}H-NMR (300 MHz, $CDCl_3$): 4.01–4.06 (*m*, 8 H); 4.21–4.25 (*m*, 8 H); 6.92 (*d*, *J* = 8.4, 2 H); 7.37 (*d*, *J* = 1.9, 2 H); 7.43 (*dd*, *J* = 1.9, 8.4, 2 H); 9.83 (*s*, 2 H). ^{13}C-NMR (75.5 MHz, $(CD_3)_2SO$): 65.80; 66.27; 66.78; 66.91; 108.05; 110.05; 124.49; 127.95; 146.61; 151.66; 189.88. FAB-MS: 455.0 (100, [*M* + K]$^+$), 439.0 (19, [*M* + Na]$^+$), 417.0 (81, *M*H$^+$). Anal. calc. for $C_{22}H_{24}O_8$ (416.43): C 63.45, H 5.81, O 30.74; found: C 63.31, H 5.95, O 30.74.

*6,7,9,10,17,18,20,21-Octahydrodibenzo[*b,k*][1,4,7,10,13,16]hexaoxacyclooctadecin-2,13-dimethanol* (**7**). $NaBH_4$ (0.82 g, 21.1 mmol) was added to a suspension of **6** (1.1 g, 2.6 mmol) in MeOH (300 ml) at 0°. After stirring for 1 h at r.t., the mixture was partitioned between H_2O and AcOEt and the org. layer was dried ($MgSO_4$) and evaporated *in vacuo* to give **7** (0.8 g, 72%). White solid. M.p. 166–169° (MeOH/$CHCl_3$). IR (KBr): 3385*m* (br.), 2921*w*, 2879*w*, 1594*w*, 1518*s*, 1429*m*, 1258*s*, 1168*w*, 1138*s*, 1052*m*, 962*m*, 806*w*. ^{1}H-NMR (300 MHz, CD_3OD): 3.94–3.97 (*m*, 8 H); 4.13–4.18 (*m*, 8 H); 4.51 (*s*, 4 H); 6.88–6.96 (*m*, 6 H). ^{13}C-NMR

(75.5 MHz, CD_3OD): 65.27; 69.73; 69.83; 71.11 (2×); 113.62; 114.28; 121.18; 136.16; 149.55; 150.22. FAB-MS: 459.1 (7, $[M+K]^+$), 443.0 (53, $[M+Na]^+$), 420.1 (100, M^+), 403.1 (75, $[M-OH]^+$).

*1,1′-Diethyl 3,3′-[(6,7,9,10,17,18,20,21-Octahydrodibenzo[*b,k*][1,4,7,10,13,16]hexaoxacyclooctadecin-2,13-diyl)dimethylene] Bis(malonate)* (**4**). To a suspension of **7** (250 mg, 0.6 mmol) and pyridine (0.14 ml, 1.8 mmol) in CH_2Cl_2 (10 ml) at 0°, EtO_2CCH_2COCl (0.24 ml, 1.8 mmol) was added, and the mixture was stirred for 1 h. After stirring for 2 h at r.t., the mixture was washed (H_2O), dried ($MgSO_4$), and concentrated *in vacuo*. FC (SiO_2-*H*; CH_2Cl_2/AcOEt 1:1) provided **4** (267 mg, 69%). White powder. M.p. 108–110° (CH_2Cl_2/AcOEt). IR (KBr): 2944*w*, 1732*s* (br.), 1518*s*, 1432*w*, 1332*m*, 1265*s* (br.), 1141*s*, 1061*w*, 1032*w*, 958*w*, 804*w*. ^{1}H-NMR (300 MHz, $CDCl_3$): 1.24 (*t*, *J* = 7.2, 6 H); 3.39 (*s*, 4 H); 3.97–4.03 (*m*, 8 H); 4.14–4.22 (*m*, 12 H); 5.09 (*s*, 4 H); 6.81–6.88 (*m*, 6 H). ^{13}C-NMR (75.5 MHz, $CDCl_3$): 14.06; 41.73; 61.64; 67.32; 68.95; 69.05; 69.99 (2×); 113.46; 114.27; 122.00; 128.51; 149.02; 149.29; 166.80 (2×). FAB-MS: 671 (13, $[M+Na]^+$), 648.1 (100, M^+), 517.1 (88, $[M-C_5H_7O_4]^+$). Anal. calc. for $C_{32}H_{40}O_{14}$ (648.66): C 59.25, H 6.22, O 34.53; found: C 59.38, H 6.28, O 34.34.

(±)-out,out-*61,62-Diethyl 61,62-[(6,7,9,10,17,18,20,21-Octahydrodibenzo[*b,k*][1,4,7,10,13,16]hexaoxacyclooctadecin-2,13-diyl)dimethylene] 1,2:55,60-Bismethano[60]fullerene-61,61,62,62-tetracarboxylate* ((±)-**1**) *and (±)*-out,out-*61,62-Diethyl 61,62-[(6,7,9,10,17,18,20,21-Octahydrodibenzo[*b,k*][1,4,7,10,13,16]hexaoxacyclooctadecin-2,13-diyl)dimethylene] 1,2:51,52-Bismethano[60]fullerene-61,61,62,62-tetracarboxylate* ((±)-**2**). DBU (69 µl, 0.462 mmol) in CH_2Cl_2 (1 ml) was injected dropwise at r.t. to a soln. of C_{60} (56 mg, 0.077 mmol), I_2 (39 mg, 0.154 mmol), [2.2.2]cryptand (6 mg, 0.016 mmol), and **4** (50 mg, 0.077 mmol) in PhMe (50 ml), and the mixture was stirred for 6 h. The soln. was extracted with H_2O, dried ($MgSO_4$), and filtered through a short plug (SiO_2-*H*) to elute residual C_{60} with PhMe, then the macrocyclic bis-adducts with AcOEt/PhMe 1:1. FC (SiO_2-*H*; PhMe/AcOEt 1:1) provided (±)-**2** (3 mg, 3%) and (±)-**1** (31 mg, 30%), in addition to a third non-characterized fraction containing at least 3 other bis-adducts (8 mg, 8%).

Data of (±)-**1**: Dark yellow solid. M.p. >250° (hexane/CH_2Cl_2). UV/VIS (CH_2Cl_2): 254 (sh, 96500), 263 (96900), 324 (38500), 405 (sh, 5500), 441 (3000), 464 (sh, 3600), 470 (3800), 540 (sh, 800), 593 (sh, 500), 640 (sh, 200). IR (KBr): 2911*m*, 1743*s*, 1516*m*, 1456*w*, 1361*w*, 1250*s*, 1168*m*, 1141*m*, 1063*m*, 857*w*, 802*w*, 735*w*, 668*m*, 524*w*. ^{1}H-NMR (300 MHz, $CDCl_3$): 1.58 (*t*, *J* = 7.2, 6 H); 3.71–4.17 (*m*, 16 H); 4.67 (*q*, *J* = 7.2, 4 H); 5.40 (*d*, *J* = 10.6, 2 H); 5.81 (*d*, *J* = 10.6, 2 H); 6.64 (*d*, *J* = 8.4, 2 H); 6.93 (*d*, *J* = 1.6, 2 H); 7.09 (*dd*, *J* = 8.4, 1.6, 2 H). ^{13}C-NMR (125.8 MHz, $CDCl_3$): 14.36; 45.29; 53.38; 63.57; 67.95; 68.67; 69.43; 69.63; 69.86; 70.13; 112.08; 114.18; 124.37; 127.88; 136.99; 137.77; 140.50 (2×); 140.63; 140.95; 141.08; 141.10; 142.13; 142.38; 142.66; 143.17; 143.25; 143.27; 143.35; 143.64 (2×); 143.80; 144.35; 144.42; 144.63; 144.75; 145.03; 145.28; 145.30 (2×); 148.13; 149.34; 164.36; 164.46 (2 signals missing due to overlap). FAB-MS: 1403.8 (17, $[M+K]^+$), 1387.9 (46, $[M+Na]^+$), 1364.9 (100, M^+, $^{13}C^{12}C_{91}H_{36}O_{14}^+$). HR-ESI-FT-MS: 1387.2010 ($[M+Na]^+$, $C_{92}H_{36}NaO_{14}^+$; calc. 1387.1997). X-Ray analysis of 1:1 complex with KPF_6: see *Fig. 3*.

Data of (±)-**2**: Dark orange solid. M.p. >250° (hexane/CH_2Cl_2). UV/VIS (CH_2Cl_2): 263 (57500), 312 (sh, 19600), 371 (sh, 5900), 400 (sh, 2900), 430 (2070), 465 (sh, 1100), 555 (sh, 600), 631 (300), 696 (200). ^{1}H-NMR (500 MHz, $(CDCl_2)_2$, 392 K): 1.59 (*t*, *J* = 7.1, 6 H); 3.67–4.04 (*m*, 16 H); 4.68 (*q*, *J* = 7.1, 4 H); 5.29 (*d*, *J* = 9.4, 2 H); 5.44 (*d*, *J* = 9.4, 2 H); 6.58 (*d*, *J* = 6.0, 2 H); 6.86 (*d*, *J* = 6.0, 2 H); 7.08 (*s*, 2 H). ^{13}C-NMR (125.8 MHz, $CDCl_3$): 14.30; 49.84; 63.57; 67.26; 68.63; 68.83; 69.60; 70.10; 70.59; 71.39; 111.93; 114.57; 122.56; 127.84; 135.93; 136.47; 139.71; 140.94; 141.48; 141.73; 141.79; 142.08; 142.16; 142.18; 142.38; 142.58; 142.74; 143.50; 143.53; 143.66; 143.73; 143.93; 144.36; 144.67; 144.77; 144.97; 145.25 (2×); 145.28; 145.98; 146.01; 146.92; 147.31; 148.06; 148.51; 162.64; 163.60. FAB-MS: 1403.8 (14, $[M+K]^+$), 1387.9 (43, $[M+Na]^+$), 1364.8 (88, M^+). HR-FAB-MS: 1364.2104 (M^+, $C_{92}H_{36}O_{14}^+$; calc. 1364.2105).

Regioselective Synthesis of (±)-**1** *Templated by K^+ Ions.* To **4** (50 mg, 0.077 mmol), I_2 (39 mg, 0.154 mmol), and C_{60} (56 mg, 0.077 mmol) in PhMe (110 ml), KPF_6 (142 mg, 0.77 mmol) in MeCN (5 ml) was added, followed by dropwise injection of DBU (69 µl, 0.462 mmol) in CH_2Cl_2 (1 ml). After stirring for 6 h, the soln. was washed (H_2O), dried ($MgSO_4$), and chromatographed (SiO_2-*H*), eluting first with PhMe to recover unreacted C_{60} (17 mg, 16%), then with PhMe/AcOEt 1:1 to give (±)-**1** (52 mg, 50%) as the only isolable bis-adduct.

*Mixture of 6,7,9,10,17,18,20,21-Octahydrodibenzo[*b,k*][1,4,7,10,13,16]hexaoxacyclooctadecin-2,14-dicarbaldehyde* (**8**) *and* **6**. A soln. of dibenzo[18]crown-6 (10.0 g, 27.2 mmol), hexamethylenetetramine (15.2 g, 108.8 mmol), and CF_3COOH (43 ml) was stirred at 115° under N_2 for 24 h. After addition of H_2O (500 ml), the mixture was extracted with PhMe, and the org. phase was dried ($MgSO_4$) and evaporated *in vacuo*. FC (SiO_2; $CHCl_3$/MeOH 99:1) afforded **6**/**8** 1:1 (2.4 g, 21%) which was not separated. White powder. IR (KBr): 2947*w*, 2922*w*, 2872*w*, 1688*s*, 1612*s*, 1587*s*, 1512*s*, 1438*s*, 1268*s*, 1165*m*, 1137*s*, 1055*w*, 999*w*, 925*w*, 868*w*, 806*w*, 742*w*, 655*w*. ^{1}H-NMR (300 MHz, $CDCl_3$): 4.00–4.06 (*m*, 8 H); 4.21–4.25 (*m*, 8 H); 6.93 (*d*, *J* = 8.1, 2 H); 7.37 (*d*, *J* = 1.9, 2 H); 7.43 (*dd*, *J* = 1.9, 8.1, 2 H); 9.83 (*s*, 2 H). ^{13}C-NMR (75.5 MHz, $CDCl_3$): 68.31; 68.39; 68.45; 68.52; 69.44; 69.52; 69.60; 110.32; 111.60; 127.07; 127.26; 130.43; 130.48; 149.21; 154.20; 191.24. FAB-MS: 455.0 (5, $[M+$

K]$^+$), 439.0 (26, [M + Na]$^+$), 417.0 (100, MH$^+$). Anal. calc. for $C_{22}H_{24}O_8$ (416.43): C 63.45, H 5.81, O 30.74; found: C 63.44, H 6.03, O 30.53.

*Mixture of 6,7,9,10,17,18,20,21-Octahydrodibenzo[*b,k*][1,4,7,10,13,16]hexaoxacyclooctadecin-2,14-dimethanol* (**9**) *and* **7**. $NaBH_4$ (0.63 g, 16.6 mmol) was added to **6**/**8** 1:1 (2.3 g, 5.5 mmol) in $CHCl_3$ (250 ml), and the soln. was stirred for 36 h at r.t. The formed white solid was filtered off, dissolved in MeOH, and neutralized with CF_3COOH. The soln. was partitioned between H_2O and AcOEt, and the org. layer was dried ($MgSO_4$) and evaporated *in vacuo* to give **7**/**9** 1:1 (1.2 g, 52%). White solid. IR (KBr): 3374*m* (br.), 2922*w*, 2877*w*, 1593*w*, 1518*s*, 1430*m*, 1328*w*, 1260*s*, 1168*m*, 1137*s*, 1062*w*, 961*w*, 795*w*. ^{1}H-NMR (300 MHz, CD_3OD): 3.97–3.99 (*m*, 8 H); 4.14–4.18 (*m*, 8 H); 4.53 (*s*, 4 H); 6.86–6.98 (*m*, 6 H). ^{13}C-NMR (50.3 MHz, CD_3OD): 63.67; 68.12; 69.48 (2×); 111.79; 112.43; 119.54; 134.49; 147.82; 148.45. FAB-MS: 459 (39, [M + K]$^+$, 443.0 (100, [M + Na]$^+$), 420.1 (98, M^+), 403.1 (88, [M – OH]$^+$).

*Mixture of 1,1′-Diethyl 3,3′-[(6,7,9,10,17,18,20,21-Octahydrodibenzo[*b,k*][1,4,10,13,16]hexaoxacyclooctadecin-2,14-diyl)dimethylene] Bis(malonate)* (**10**) *and* **4**. Et_3N (0.3 ml, 2.10 mmol) was added *via* syringe over 5 min at 0° to **7**/**9** 1:1 (0.4 g, 0.95 mmol), then EtO_2CCH_2COCl (0.28 g, 2.10 mmol) in DMF (15 ml, dried over 4-Å molecular sieves) was added in the same way. The soln. was stirred for 1 h at 0°, then for 2 h at r.t., after which it was neutralized with CF_3COOH and evaporated *in vacuo*. FC (SiO_2-*H*; CH_2Cl_2/AcOEt 1:1) gave **4**/**10** 1:1 (450 mg, 74%). White solid. IR (KBr): 2944*w*, 1778*s*, 1728*s*, 1519*s*, 1432*w*, 1336*m*, 1267*s*, 1142*s*, 1061*w*, 1032*w*, 971*w*, 805*w*. ^{1}H-NMR (300 MHz, $CDCl_3$): 1.24 (*t*, *J* = 7.2, 6 H); 3.39 (*s*, 4 H); 3.89–4.02 (*m*, 8 H); 4.14–4.21 (*m*, 12 H); 5.09 (*s*, 4 H); 6.81–6.91 (*m*, 6 H). ^{13}C-NMR (75.5 MHz, $CDCl_3$): 14.06; 41.73; 61.64; 67.34; 69.00; 69.97; 113.43; 114.20; 121.95; 128.47; 149.02; 149.28; 166.77. FAB-MS: 671.1 (7, [M + Na]$^+$), 648.1 (100, M^+), 517.1 (55, [M – $C_5O_4H_7$]$^+$). Anal. calc. for $C_{32}H_{40}O_{14}$ (648.66): C 59.25, H 6.22, O 34.53; found: C 59.24, H 6.18, O 34.58.

*(±)-*in,out-*61,62-Diethyl 61,62-[(6,7,9,10,17,18,20,21-Octahydrodibenzo[*b,k*][1,4,7,10,13,16]hexaoxacyclooctadecin-2,13-diyl)dimethylene] 1,2 : 33,50-Bismethano[60]fullerene-61,61,62,62-tetracarboxylate* ((±)-**3**). DBU (0.5 ml, 3.36 mmol) was added dropwise at r.t. to a soln. of C_{60} (400 mg, 0.56 mmol), I_2 (310 mg, 1.22 mmol), and **4** (396 mg, 0.61 mmol) in PhMe (400 ml), and the mixture was stirred for 14 h. Filtration through a short plug (SiO_2) eluting first with PhMe to remove unreacted C_{60}, then with PhMe/AcOEt 1:1 afforded a mixture of macrocyclic bis-adducts. FC (SiO_2-*H*; AcOEt/PhMe 1:1) provided, in the order of elution, (±)-**2** (12 mg, 1.5%), (±)-**3** (151 mg, 20%), (±)-**1** (113 mg, 15%), and a fourth fraction containing at least 3 unidentified products (37 mg, 5%). Dark red solid. M.p. > 250° (hexane/CH_2Cl_2). UV/VIS (CH_2Cl_2): 263 (sh, 76100), 309 (sh, 32700), 329 (sh, 24500), 391 (sh, 6200), 398 (sh, 5800), 411 (4300), 421 (3300), 489 (2500), 556 (sh, 1400), 612 (sh, 600), 668 (sh, 200). IR (KBr): 2922*m*, 1745*s*, 1516*m*, 1428*w*, 1378*w*, 1251*s* (br.), 1167*m*, 1141*m*, 1058*m*, 856*w*, 800*w*, 667*m*, 528*m*. ^{1}H-NMR (500 MHz, $(CDCl_2)_2$, 333 K): 1.36 (*t*, *J* = 7.1, 3 H); 1.44 (*t*, *J* = 7.1, 3 H); 3.75–4.07 (*m*, 16 H); 4.39–4.43 (*m*, 2 H); 4.49–4.52 (*m*, 2 H); 4.95 (*d*, *J* = 11.1, 1 H); 5.45 (*s*, 2 H); 5.66 (*d*, *J* = 11.1, 1 H); 6.51 (*d*, *J* = 8.0, 1 H); 6.78 (*d*, *J* = 8.1, 1 H); 6.88–6.91 (*m*, 3 H); 7.10 (*dd*, *J* = 8.1, 1.6, 1 H). ^{13}C-NMR (125.8 MHz, $(CDCl_2)_2$, 333 K): 14.48; 14.56; 51.38; 52.17; 63.74; 63.80; 68.70; 68.99; 69.19; 69.38; 69.46; 69.54; 69.62; 69.82; 69.92; 70.07; 71.34; 71.73; 71.82; 72.21; 112.63; 113.05; 116.50; 116.73; 124.02; 124.70; 127.84; 128.39; 136.06; 138.12; 139.28; 139.70; 140.02; 140.32; 141.15; 141.40; 141.74; 141.84; 141.95; 142.02; 142.24; 142.52; 143.07; 143.10; 143.16; 143.21; 143.30; 143.40; 143.44; 143.48; 143.56; 143.58; 143.74; 143.89; 144.06; 144.21; 144.48; 144.52; 144.65; 144.71; 145.19; 145.21; 145.33; 145.38; 145.52; 145.77; 145.83; 145.90; 145.94; 146.15; 146.26; 146.33; 146.57; 146.65; 146.85; 146.97; 147.08; 147.46; 147.98; 148.74; 149.56; 150.00; 163.15; 163.49; 163.63; 164.40 (6 C missing due to signal overlap). FAB-MS: 1403.8 (21, [M + K]$^+$), 1387.9 (100, [M + Na]$^+$), 1364.9 (49, $^{13}C^{12}C_{91}H_{36}O_{13}^+$). HR-FAB-MS: 1364.2101 (M^+, $C_{92}H_{36}O_{14}^+$; calc. 1364.2105).

Tetrahexyl 1,2 : 55,60-Bismethano[60]fullerene-61,61,62,62-tetracarboxylate (**11**). *Method A*. A mixture of (±)-**1** (10 mg, 0.007 mmol) and KPF_6 (14 mg, 0.07 mmol) in hexanol/THF 1:1 (10 ml) was sonicated for 10 min, then Cs_2CO_3 (73 mg, 0.22 mmol) was added. After stirring for 3.5 h, the reaction was quenched with 1% aq. CF_3COOH soln. and the org. layer was washed (H_2O), dried ($MgSO_4$), and evaporated *in vacuo*. FC (SiO_2-*H*; CH_2Cl_2/hexane 1:1) yielded **11** (3 mg, 34%).

Method B. A soln. of (±)-**12** (10 mg, 0.007 mmol) and $TsOH \cdot H_2O$ (53 mg, 0.279 mmol) in PhMe (4 ml) was heated to reflux for 12 h. The brown precipitate of **14** formed was recovered by centrifugation, washed with PhMe, dried, then washed again with H_2O and dried. To a suspension of crude **14** in dry CH_2Cl_2 (1.5 ml), $(COCl)_2$ (0.2 ml) was added *via* syringe. The mixture was heated to 40° and stirred under Ar for 4 h. Excess $(COCl)_2$ was removed by vacuum distillation, and the residual crude **15** was dried in high vacuum. This solid was suspended in dry CH_2Cl_2 (2 ml), hexanol (10 µl, 0.08 mmol), and pyridine (5 µl, 0.06 mmol), and the mixture was stirred overnight. The resulting soln. was washed with 1% aq. CF_3COOH soln. and H_2O, dried ($MgSO_4$), and evaporated *in vacuo*. FC (SiO_2-*H*; hexane/CH_2Cl_2 4:1) gave **11** (4.1 mg, 45%), which was eluted after a

fraction containing the corresponding tris(hexyl ester) (2 mg, 20%). Black solid. M.p. >250° (CH_2Cl_2/hexane). UV/VIS (CH_2Cl_2): 256 (100900), 323 (40500), 367 (sh, 11800), 408 (sh, 4600), 429 (2400), 440 (2800), 468 (sh, 3600), 470 (3900), 539 (sh, 800), 585 (sh, 500) 640 (sh, 200). IR ($CHCl_3$): 3689*w*, 2944*m*, 2922*m*, 2856*w*, 1739*m*, 1600*w*, 1467*w*, 1378*w*, 1256*s*, 1188*w*, 1172*w*, 1083*w*, 1006*w*, 906*w*, 833*w*, 572*w*, 528*m*. ^{1}H-NMR (300 MHz, $CDCl_3$): 0.91–0.95 (*m*, 12 H); 1.33–1.43 (*m*, 16 H); 1.51–1.57 (*m*, 8 H); 1.89–1.94 (*m*, 8 H); 4.59 (*t*, *J* = 6.5, 8 H). ^{13}C-NMR (125.8 MHz, $CDCl_3$): 13.84; 22.41; 25.49; 28.42; 31.22; 45.89; 67.36; 70.07; 138.93; 141.03; 143.31; 143.41; 143.45; 144.64; 145.05; 145.22; 164.02. FAB-MS: 1261.8 (1, M^+), 720.0 (100, C_{60}^+). HR-FAB-MS: 1260.3673 (M^+, $C_{90}H_{52}O_8^+$; calc. 1260.3662).

*1,1′-Di(*tert*-butyl) 3,3′-[(6,7,9,10,17,18,20,21-Octahydrodibenzo[*b,k*][1,4,7,10,13,16]hexaoxacyclooctadecin-2,13-diyl)dimethylene] Bis(malonate)* (**13**). $(COCl)_2$ (0.42 ml, 4.8 mmol) was added at 0° to a soln. of *t*-BuO_2CCH_2COOH (600 mg, 3.6 mmol) and pyridine (0.29 ml, 3.6 mmol) in CH_2Cl_2 (10 ml). After stirring for 1 h at r.t., unreacted $(COCl)_2$ was distilled off, and the residue was dissolved in dry CH_2Cl_2. The resulting soln. was added over 5 min *via* syringe to a suspension of **7** (500 mg, 1.19 mmol) in pyridine (0.29 ml, 3.6 mmol) and CH_2Cl_2 (50 ml). After stirring for 1 h, the mixture was washed with sat. aq. $NaHCO_3$ soln., 1% aq. CF_3COOH soln., H_2O, dried ($MgSO_4$), and evaporated. FC (SiO_2-*H*; CH_2Cl_2/AcOEt 1:1) afforded **13** (440 mg, 52%). White solid. M.p. 97–98° (CH_2Cl_2/AcOEt). IR (KBr): 3432*m* (br.), 2966*m*, 2933*m*, 2878*m*, 1728*s*, 1611*w*, 1594*m*, 1517*s*, 1456*m*, 1428*m*, 1367*s*, 1333*s*, 1261*s*, 1172*s*, 1139*s*, 1061*m*, 972*m*, 956*m*, 922*w*, 844*w*, 800*m*, 750*w*, 633*w*, 549*w*, 539*w*, 506*w*, 461*w*. ^{1}H-NMR (300 MHz, $CDCl_3$): 1.42 (*s*, 18 H); 3.30 (*s*, 4 H); 4.00–4.04 (*m*, 8 H); 4.14–4.18 (*m*, 8 H); 5.08 (*s*, 4 H); 6.81–6.92 (*m*, 6 H). ^{13}C-NMR (75.5 MHz, $CDCl_3$): 27.96; 43.02; 67.17; 68.92; 69.04; 69.97; 76.74; 82.24; 113.41; 114.24; 122.00; 128.59; 149.00; 149.25; 165.97; 167.02. FAB-MS: 727 (6, $[M+Na]^+$), 704 (100, M^+). Anal. calc. for $C_{36}H_{48}O_{14}$ (704.78): C 61.35, H 6.86, O 31.78; found: C 61.38, H 6.66, O 31.96.

(±)-out,out-*61,62-Di(*tert*-butyl) 61,62-[(6,7,9,10,17,18,20,21-Octahydrodibenzo[*b,k*][1,4,7,10,13,16]hexaoxacyclooctadecin-2,13-diyl)dimethylene] 1,2:55,60-Bismethano[60]fullerene-61,61,62,62-tetracarboxylate* ((±)-**12**). KPF_6 (261 mg, 1.41 mmol) in MeCN (50 ml) was added to **12** (100 mg, 0.141 mmol), I_2 (79 mg, 0.310 mmol), and C_{60} (102 mg, 0.141 mmol) in PhMe (500 ml). DBU (127 µl, 0.846 mmol) in CH_2Cl_2 (10 ml) was injected dropwise *via* syringe, and the mixture was stirred for 1 h. The soln. was washed (H_2O), dried ($MgSO_4$), and passed through a short SiO_2-*H* column which was eluted first with PhMe to remove unreacted C_{60} and then with PhMe/AcOEt 1:1 to give (±)-**13** (109 mg, 54%) as the only isolable regioisomer. Black solid. M.p. >250° (hexane/CH_2Cl_2). UV/VIS (CH_2Cl_2): 285 (99100), 326 (82400), 404 (sh, 5700), 442 (3000), 472 (3800), 581 (sh, 500), 639 (sh, 300). IR (KBr): 3433*m* (br.), 2967*m*, 2922*m*, 2867*m*, 1739*s*, 1717*s*, 1633*w*, 1595*w*, 1517*m*, 1450*w*, 1422*w*, 1361*m*, 1261*s*, 1145*s*, 1061*s*, 956*w*, 850*w*, 806*w*, 744*w*, 700*w*, 656*w*, 578*w*, 522*w*. ^{1}H-NMR (300 MHz, $CDCl_3$): 1.78 (*s*, 18 H); 3.73–4.21 (*m*, 16 H); 5.41 (*d*, *J* = 10.9, 2 H); 5.78 (*d*, *J* = 10.9, 2 H); 6.65 (*d*, *J* = 8.1, 2 H); 6.94 (*d*, *J* = 1.9, 2 H); 7.10 (*dd*, *J* = 1.9, 8.1, 2 H). ^{13}C-NMR (125.8 MHz, $CDCl_3$): 28.24; 46.35; 53.41; 67.89; 68.51; 69.19; 69.56; 69.71; 69.86; 70.10; 111.92; 114.09; 124.30; 127.91; 136.86; 137.67; 140.28; 140.44; 140.47; 140.89; 141.02; 141.03; 142.25; 142.56; 142.91; 143.13; 143.19; 143.25; 143.27; 143.54; 143.55; 143.61; 143.93; 144.34; 144.37; 144.47; 144.52; 144.66; 145.05; 145.29; 145.33; 145.37; 148.02; 149.21; 163.35; 164.62. FAB-MS: 1444.1 (40, $[M+Na]^+$), 1388.0 (59, $[M+Na-(t\text{-}Bu)]^+$), 1332.4 (10, $[M+Na-2\,(t\text{-}Bu)]^+$). HR-ESI-FT-MS: 1443.2628 ($[M+Na]^+$, $C_{96}H_{44}NaO_{14}^+$; calc. 1443.2623).

cis-*61,62-Diethyl 61,62-Bis(2-[2-[2-(methoxy)ethoxy]ethoxy]ethyl) 1,2:55,60-Bismethano[60]fullerene-61,61,62,62-tetracarboxylate* (**18**). $TsOH \cdot H_2O$ (28 mg, 0.15 mmol) was added to (±)-**1** (10 mg, 0.007 mmol) in PhMe (3 ml), and the mixture was heated to reflux for 3 h. Dicarboxylic acid **16** precipitated as a brown solid, which was recovered by centrifugation, washed with PhMe and H_2O, and dried under high vacuum. $(COCl)_2$ (0.5 ml) was added *via* syringe to a suspension of crude **16** in dry CH_2Cl_2 (2 ml), and the mixture was stirred at 40° under Ar for 2 h. Excess $(COCl)_2$ was removed by vacuum distillation, and crude **17** was obtained as a brown solid and was dried under high vacuum. This solid was suspended in a soln. of dry CH_2Cl_2 (2 ml), triethyleneglycol monomethyl ether (3.5 µl, 0.021 mmol), and pyridine (1.7 µl, 0.021 mmol), and the mixture was stirred for 14 h. The resulting soln. was washed with 1% aq. CF_3COOH soln. and H_2O, dried ($MgSO_4$), and evaporated *in vacuo*. FC (SiO_2-*H*; CH_2Cl_2/AcOEt 1:1) gave **18** (6.3 mg, 68%). Black solid. M.p. >250° (CH_2Cl_2/Hexane). UV/VIS (CH_2Cl_2): 281 (51000), 324 (42000), 403 (sh, 2300), 440 (1300), 463 (sh, 1600), 470 (2100), 531 (sh, 300), 578 (sh, 300), 639 (sh, 100). IR (KBr): 3444*m* (br.), 2856*m*, 2922*m*, 2867*m*, 1739*m*, 1627*w*, 1467*w*, 1383*w*, 1244*m*, 1206*w*, 1167*w*, 1106*w*, 1072*w*, 1027*w*, 878*w*, 869*s*, 733*w*, 694*w*, 681*w*, 558*w*, 522*w*. ^{1}H-NMR (300 MHz, $CDCl_3$): 1.57 (*t*, *J* = 7.2, 6 H); 3.39 (*s*, 6 H); 3.55–3.58 (*m*, 4 H); 3.66–3.71 (*m*, 8 H); 3.74–3.78 (*m*, 4 H); 3.94–3.98 (*m*, 4 H); 4.67 (*q*, *J* = 7.2, 4 H); 4.74–4.77 (*m*, 4 H). ^{13}C-NMR (125.8 MHz, $CDCl_3$): 14.10; 45.58; 58.86; 63.37; 66.10; 68.69; 69.96; 70.44; 70.49; 70.56; 71.75; 138.87; 139.10; 140.99; 141.04; 143.15; 143.32; 143.37; 143.39;

143.48; 144.63; 144.65; 145.03; 145.04; 145.19; 145.22; 163.76; 163.96. FAB-MS: 1273 (58.0, M^+), 1109 (14, $[M-O(CH_2CH_2O)_3CH_3]^+$), 720 (100, C_{60}^+). HR-FAB-MS: 1272.2410 (M^+, $C_{84}H_{40}O_{14}^+$; calc. 1272.2418).

Ion-Selective Electrode (ISE) Membranes. Reagents. The chromoionophore ETH 2439, sodium tetrakis-[3,5-bis(trifluoromethyl)phenyl]borate (NaTFPB), bis(2-ethylhexyl) sebacate (DOS), poly(vinyl chloride) (PVC), and THF were purchased from *Fluka*. Aq. solns. were prepared with deionized water (specific resistance 18.0 M$\Omega\cdot$cm, *NANOpure*^{TM}, *Barnstead*, CH-4009 Basel). The chloride salts, LiOH, CsOH, KOAc, NaOAc, and AcOH were of *p.a.* grade from *Fluka* or *Merck*, and NaOH and KOH *Titrisol* (*Merck*) were used.

Membranes. Ion-selective electrode (ISE) membranes contained either (±)-**1** (0.86 wt-%, 6.3 mmol kg^{-1}), ETH 2439 (0.49 wt-%, 6.6 mmol kg^{-1}), NaTFPB (0.28 wt-%, 3.1 mmol kg^{-1}), DOS (66.5 wt-%), and PVC (30.0 wt-%), or (±)-**1** (1.00 wt-%, 7.4 mmol kg^{-1}), NaTFPB (0.33 wt-%, 3.3 mmol kg^{-1}), DOS (65.6 wt-%), and PVC (33.1 wt-%), or ETH 2439 (0.49 wt-%, 6.6 mmol kg^{-1}), NaTFPB (0.29 wt-%, 3.3 mmol kg^{-1}), DOS (68.0 wt-%), and PVC (31.2 wt-%). Membranes of 200 μm thickness were obtained by casting a soln. of 200–280 mg of the membrane components, dissolved in THF (*ca.* 2.5 ml), into a glass ring (26 mm i.d.) fixed on a glass plate.

Electrodes. All ISEs were prepared with *Philips IS 561* electrode bodies (*Glasbläserei Möller*, CH-8050 Zürich). The internal filling soln. was 0.01M KCl for ISE membranes based on (±)-**1** as the only ionophore, and 0.1M KCl buffered to pH 3.9 with 0.005M AcOH/AcOK for the other two. Before measurements, the ISEs were conditioned in the respective internal filling soln. overnight.

EMF Measurements. Measuring solns. were prepared by successive automatic dilution of stock solns. under full computer control in a 50-ml polyethylene beaker with the help of *Liquino 711* and *Dosino 700* (*Metrohm AG*, CH-9010 Herisau) equipped with 50-ml burettes. A custom-made 16-channel electrode monitor with an adapted *LabView* ® program was used for EMF measurements in solns. stirred with a rod stirrer at r.t. (20–21°), the reference electrode being Ag/AgCl (*Metrohm*, type *6.0729.100*) with 1M LiOAc as bridge electrolyte. Activity coefficients were calculated according to the *Debye-Hückel* approximation [43]. All EMF values (median of the potentials measured during 10 min) were corrected for liquid-junction potentials with the *Henderson* equation [44]. Selectivity coefficients were determined by the separate soln. method [32] in metal-chloride solns. For the two measuring (K^+, H^+) and each interfering cation, a calibration curve was taken (*Fig. 2*) and used for obtaining the selectivity coefficients (Cl^- salt solns.) as follows: The standard potential of the cell, E_J^0, for pure solns. of any interfering cation (J) was calculated from the linear regression of potential *vs.* activity of the cation and inserted, together with the corresponding value, E_I^0, and slope, s_I, for the measuring cation (I), into *Eqn. 1* for determining the potentiometric selectivity coefficients, log K_{IJ}^{pot}:

$$\log K_{IJ}^{pot} = \frac{E_J^0 - E_J^0}{s_I} \tag{1}$$

Effective complex formation constants, K_{IL}^{eff}, were calculated from the $K_{H,J}^{pot}$ values of two ISEs based on ETH 2439 (measured at pH 11.0), one with and the other without ligand (±)-**1** (L) according to:

$$K_{IL}^{eff} = \frac{1}{L_T - R_T^-} \; \frac{K_{H,J}^{pot}\ (\text{with L})}{K_{HJ}^{pot}\ (\text{without L})} \tag{2}$$

A 1:1 stoichiometry of the complex IL was assumed; L_T and R_T^- are the total concentrations of (±)-**1** and NaTFPB, respectively [33]. Standard deviations were calculated from the results of three ISEs prepared from the same membrane.

*X-Ray Crystal-Structure Analysis of (±)-***1** ($C_{92}H_{36}O_{14}\cdot KPF_6$)$\cdot$($CH_2Cl_2$)$\cdot$1/2($C_6H_6$) ($M_r$ = 1673.3): monoclinic space group *C*2/*c* (no. 15), D_c = 1.654 g$\cdot$cm^{-3}, Z = 8, a = 53.556(7), b = 10.091(2), c = 27.297(4) Å, β = 114.39(1)°, V = 13436(4) Å^3. Black, plate-like single crystals were obtained by slow evaporation of a CH_2Cl_2/PhH soln. The X-ray measurements were carried out on a *Nonius CAD4* diffractometer with CuK_α radiation (λ = 1.5418 Å) at 243 K. The structure was solved by direct methods (SIR92) [45] and refined by full-matrix least-squares analysis (SHELXL-97) [46], with an isotropic extinction correction and $w = 1/[\sigma^2(F_o^2) + (0.1228P)^2 + 198.7522P]$, where $P = (F_o^2 + 2F_c^2)/3$. Substantial disorder occurs for one ethyl-malonate subunit (C(92) to C(101)), the PF_6 anion, and both solvent molecules. The disorder could be resolved for the atoms C(92), O(93), O(95), O(99), C(100), C(101), and the F-atoms (*Fig. 3*). For the former (C and O) atoms, two sets of atomic parameters were refined (mostly isotropically) with population parameters (pp) of 0.5. For the latter (F), two sets of parameters were refined anisotropically with pp of 0.5; corresponding P–F and F–F distances were restrained to preserve an approximate octahedral symmetry. The CH_2Cl_2 is disordered over at least two orientations; in the present analysis, two sets of atomic paramters with pp of 0.5 were refined isotropically. The benzene (lying on a crystallographic twofold axis) was refined anisotropically with pp of 0.5. The geometry of both solvents is highly distorted. All other heavy atoms were refined anisotropically (H-atoms of the ordered

skeleton isotropically, whereby H-positions are based on stereochemical considerations). Final $R(F) = 0.078$, $wR(F^2) = 0.20$ for 1140 parameters, 28 restraints, and all 4774 reflections with $I > 2\sigma(I)$ and $1.81 < \theta < 52^\circ$ (corresponding R values with all 7517 observed reflections are 0.122 and 0.246, respectively).

Crystallographic data (excluding structure factors) for the structure reported in this paper have been deposited with the *Cambridge Crystallographic Data Centre* as deposition No. CCDC-127941. Copies of the data can be obtained, free of charge, on application to the *CCDC*, 12 Union Road, Cambridge CB2 1EZ UK (fax: + 44 (1223) 336033; e-mail: deposit@ccdc.cam.ac.uk).

Electrochemical Experiments. The measurements were performed under Ar in dry $MeCN/CH_2Cl_2$ (1:1, 5 ml) containing 0.1M Bu_4NPF_6, typically using 0.5 mM solns. of the fullerene-crown ether conjugate. The solvent mixture was selected mainly for solubility reasons. [2.2.2]Cryptand and KPF_6 were added directly to the cell as solids. An *EG & G Princeton Applied Research* Model *263A* potentiostat/galvanostat was used to obtain all of the measurements. A glassy carbon mini-electrode was used as the working electrode, an Ag/AgCl electrode from *Bioanalytical Systems* was used as the reference, and 0.5 mM Fc was added as an internal potential standard. A Pt wire served as the counter-electrode. A typical scan was run at a rate of 100 mV s^{-1}, and no soln. resistance compensation was applied.

This work was supported by the *Swiss National Science Foundation*, *F. Hoffmann-La Roche AG*, Basel, the *US National Science Foundation* (CHE-9816503), and a *NIH Fogarty Fellowship* (1F 06 TW-02231-01) to *L.E.* We thank Prof. *B. Jaun* (ETH Zürich) for help with the NMR lineshape analysis, Dr. *M. Sebova* for the VT-NMR measurements, and Dr. *C. Thilgen* for assistance with the nomenclature.

REFERENCES

[1] A. Hirsch, 'The Chemistry of the Fullerenes', Thieme, Stuttgart, 1994; F. Diederich, C. Thilgen, *Science (Washington D.C.)* **1996**, *271*, 317; A. Hirsch, *Top. Curr. Chem.* **1998**, *199*, 1.

[2] a) F. Diederich, M. Gómez-López, *Chimia* **1998**, *52*, 551; b) F. Diederich, M. Gómez-López, *Chem. Soc. Rev.*, in press.

[3] S. R. Wilson, Y. Wu, *J. Chem. Soc., Chem. Commun*. **1993**, 784; F. Arias, Q. Yie, Y. Wu, Q. Lu, S. R. Wilson, L. Echegoyen, *J. Am. Chem. Soc*. **1994**, *116*, 6388; S. N. Davey, D. A. Leigh, A. E. Moody, L. W. Tetler, F. A. Wade, *J. Chem. Soc., Chem. Commun*. **1994**, 397; A. Gügel, A. Kraus, J. Spickermann, P. Belik, K. Müllen, *Angew. Chem.* **1994**, *106*, 601; *ibid., Int. Ed*. **1994**, *33*, 559; A. Kraus, A. Gügel, P. Belik, M. Walter, K. Müllen, *Tetrahedron* **1995**, *51*, 9927; F. Arias, L. Echegoyen, S. R. Wilson, Q. Lu, Q. Lu, *J. Am. Chem. Soc*. **1995**, *117*, 1422; J. Osterodt, A. Zett, F. Vögtle, *Tetrahedron* **1996**, *52*, 4949.

[4] F. Diederich, U. Jonas, V. Gramlich, A. Herrmann, H. Ringsdorf, C. Thilgen, *Helv. Chim. Acta* **1993**, *76*, 2445; D. A. Leigh, A. E. Moody, F. A. Wade, T. A. King, D. West, G. S. Bahra, *Langmuir* **1995**, *11*, 2334; U. Jonas, F. Cardullo, P. Belik, F. Diederich, A. Gügel, E. Harth, A. Herrmann, L. Isaacs, K. Müllen, H. Ringsdorf, C. Thilgen, P. Uhlmann, A. Vasella, C. A. A. Waldraff, M. Walter, *Chem. Eur. J*. **1995**, *1*, 243; S. Wang, R. M. Leblanc, F. Arias, L. Echegoyen, *Langmuir* **1997**, *13*, 1672.

[5] J. Osterodt, M. Nieger, P.-M. Windscheif, F. Vögtle, *Chem. Ber*. **1993**, *126*, 2331; A. Ikeda, C. Fukuhara, S. Shinkai, *Chem. Lett*. **1997**, 407; M. Kawaguchi, A. Ikeda, S. Shinkai, *J. Chem. Soc., Perkin Trans. 1*, **1998**, 179; Z. Guo, Y. Li, J. Xu, Z. Mao, Y. Wu, D. Zhu, *Synth. Commun.* **1998**, *28*, 1957.

[6] F. Arias, L. A. Godinez, S. R. Wilson, A. E. Kaifer, L. Echegoyen, *J. Am. Chem. Soc*. **1996**, *118*, 6086; P. R. Ashton, F. Diederich, M. Gómez-López, J.-F. Nierengarten, J. A. Preece, F. M. Raymo, J. F. Stoddart, *Angew. Chem.* **1997**, *109*, 1611; *ibid., Int. Ed*. **1997**, *36*, 1448; F. Diederich, L. Echegoyen, M. Gómez-López, R. Kessinger, J. F. Stoddart, *J. Chem. Soc., Perkin Trans. 2*, in press.

[7] L. Echegoyen, L. E. Echegoyen, *Acc. Chem. Res.* **1998**, *31*, 593.

[8] J.-F. Nierengarten, V. Gramlich, F. Cardullo, F. Diederich, *Angew. Chem.* **1996**, *108*, 2242; *ibid., Int. Ed*. **1996**, *35*, 2101; J.-F. Nierengarten, T. Habicher, R. Kessinger, F. Cardullo, F. Diederich, V. Gramlich, J.-P. Gisselbrecht, C. Boudon, M. Gross, *Helv. Chim. Acta* **1997**, *80*, 2238.

[9] F. Diederich, R. Kessinger, *Acc. Chem. Res.* **1999**, *32*, 537.

[10] C. Bingel, *Chem. Ber*. **1993**, *126*, 1957.

[11] a) J.-P. Bourgeois, F. Diederich, L. Echegoyen, J.-F. Nierengarten, *Helv. Chim. Acta* **1998**, *81*, 1835; b) E. Dietel, A. Hirsch, E. Eichhorn, A. Rieker, S. Hackbarth, B. Röder, *Chem. Commun*. **1998**, 1981.

[12] A. Hirsch, I. Lamparth, H. R. Karfunkel, *Angew. Chem.* **1994**, *106*, 453; *ibid., Int. Ed.* **1994**, *33*, 437.

[13] J.-P. Bourgeois, L. Echegoyen, M. Fibbioli, E. Pretsch, F. Diederich, *Angew. Chem.* **1998**, *110*, 2203; *ibid., Int. Ed.* **1998**, *37*, 2118.

[14] B. Kräutler, T. Müller, J. Maynollo, K. Gruber, C. Kratky, P. Ochsenbein, D. Schwarzenbach, H.-B. Bürgi, *Angew. Chem*. **1996**, *108*, 1294; *ibid., Int. Ed*. **1996**, *35*, 1204; Y. Rubin, *Chem. Eur. J.* **1997**, *3*, 1009.
[15] CVFF Force field in the program Insight II v. 95.0 within the Discover v. 2.9.7 package from *Biosym Technologies*, San Diego, 1997.
[16] Program Spartan SGI v. 4.0.3 GL, *Wavefunction Inc.*, Irvine, 1995.
[17] A. Reitz, M. A. Avery, M. S. Verlander, M. Goodman, *J. Org. Chem.* **1981**, *46*, 4859.
[18] C. J. Pedersen, *Org. Synth. Coll. Vol. 6*, **1972**, 395; R. N. Greene, *Tetrahedron Lett*. **1972**, 1793.
[19] a) 'Templated Organic Synthesis', Eds. F. Diederich, P. J. Stang, Wiley-VCH, Weinheim, in press; b) N. V. Gerbeleu, V. B. Arion, J. Burgess, 'Template Synthesis of Macrocyclic Compounds', Wiley-VCH, Weinheim, 1999.
[20] G. W. Gokel, 'Crown Ethers and Cryptands', The Royal Society of Chemistry, 1991.
[21] W. E. Smith, *J. Org. Chem.* **1972**, *37*, 3972.
[22] J. C. Duff, *J. Chem. Soc*. **1941**, 547.
[23] F. Wada, H. Hirayama, H. Namiki, K. Kikukawa, T. Matsuda, *Bull. Chem. Soc. Jpn*. **1980**, *53*, 1473.
[24] F. Djojo, A. Herzog, I. Lamparth, F. Hampel, A. Hirsch, *Chem. Eur. J.* **1996**, *2*, 1537.
[25] Q. Lu, D. I. Schuster, S. R. Wilson, *J. Org. Chem.* **1996**, *61*, 4764.
[26] CS Chem3D Pro v. 3.5.1, *CambridgeSoft Corporation*, Cambridge, 1997.
[27] B. Jaun, M. Tanaka, P. Seiler, F. N. M. Kühnle, C. Braun, D. Seebach, *Liebigs Ann. Chem*. **1997**, 1697.
[28] gNMR v. 3.6 for *Macintosh*, *Cherwell Scientific*, Oxford, 1995.
[29] E. Bakker, P. Bühlmann, E. Pretsch, *Chem. Rev.* **1997**, *97*, 3083.
[30] P. Bühlmann, E. Pretsch, E. Bakker, *Chem. Rev*. **1998**, *98*, 1593.
[31] E. Bakker, P. Bühlmann, E. Pretsch, *Electroanalysis*, in press.
[32] R. P. Buck, E. Lindner, *Pure Appl. Chem.* **1994**, *66*, 2527.
[33] E. Bakker, E. Pretsch, *Anal. Chem.* **1998**, *70*, 295.
[34] E. Bakker, M. Willer, M. Lerchi, K. Seiler, E. Pretsch, *Anal. Chem.* **1994**, *66*, 516.
[35] R. Taylor, *J. Chem. Soc., Perkin Trans. 2* **1993**, 813.
[36] a) P. Dapporto, P. Paoli, I. Matijasic, L. Tusek-Bozic, *Inorg. Chim. Acta* **1996**, *252*, 383; b) L. P. Battaglia, A. Bonamartini Corradi, A. Bianchi, J. Giusti, P. Paoletti, *J. Chem. Soc., Dalton Trans.* **1987**, 1779.
[37] See also: J. W. Steed, P. C. Junk, J. L. Atwood, M. J. Barnes, C. L. Raston, R. S. Burkhalter, *J. Am. Chem. Soc*. **1994**, *116*, 10346; J. L. Atwood, L. J. Barbour, C. L. Raston, I. B. N. Sudria, *Angew. Chem*. **1998**, *100*, 1029; *ibid., Int. Ed*. **1998**, *37*, 981; K. Tsubaki, K. Tanaka, T. Kinoshita, K. Fuji, *Chem. Commun*. **1998**, 895; J. L. Atwood, L. J. Barbour, P. J. Nichols, C. L. Raston, C. A. Sandoval, *Chem. Eur. J*. **1999**, *5*, 990.
[38] J. Chen, F.-F. Cai, Q.-F. Shao, Z.-E. Huang, S.-M. Chen, *Chem. Commun.* **1996**, 1111.
[39] J. L. Atwood, *J. Inclus. Phenom*. **1985**, *3*, 13.
[40] J. C. Ma, D. A. Dougherty, *Chem. Rev.* **1997**, *97*, 1303.
[41] S. R. Miller, D. A. Gustowski, Z. Chen, G. W. Gokel, L. Echegoyen, A. E. Kaifer, *Anal. Chem.* **1988**, *60*, 2021.
[42] E. D. Glendening, D. Feller, M. A. Thompson, *J. Am. Chem. Soc*. **1994**, *116*, 10657.
[43] P. C. Meier, *Anal. Chim. Acta* **1982**, *136*, 363.
[44] W. E. Morf, 'The Principles of Ion-Selective Electrodes and of Membrane Transport', Elsevier, New York, 1981.
[45] A. Altomare, G. Cascarano, C. Giacovazzo, A. Guagliardi, M. C. Burla, G. Polidori, M. Camalli, *J. Appl. Crystallogr.* **1994**, *27*, 435.
[46] G. M. Sheldrick, SHELXL-97 Program for the Refinement of Crystal Structures, University of Göttingen, Germany, 1997.

Received July 13, 1999